Ethiopian Institute of Technology-Mekelle (EIT-M)

School of Mechanical and Industrial Engineering
Thermal and Energy Systems Chair

Development Of Solar Absorption Refrigeration System for Off-Grid Application

A Thesis Submitted in Partial Fulfilment of the Requirements for the Degree of

Master of Science in Mechanical Engineering

(Thermo-fluid Engineering)

By

Merhawit G/medhin

Advisor

Petros Gebray (Ph.D. Candidate)

November 2024 Mekelle, Ethiopia

Thermal and Energy System Chair

School of Mechanical Engineering

Ethiopian Institute of Technology-Mekelle Mekelle University, Ethiopia

Development Of Solar Absorption Refrigeration System for Off-Grid Application

By

Merhawit G/medhin

Approved By Board of Examiners

Name	Signature
Berihu Gebreyohannes (PhD)	
External Examiner	
Ashenafi Kebedom Internal Examiner	
Petros Gebray Advisor	
Zinabu Tsegazab Chair Person	

DECLARATION

I declare that this research entitled: - "Development of Solar Absorption Refrigeration System for Off-Grid Application" in the partial fulfillment of the requirement for the award of M.sc in mechanical and industrial engineering is an authentic record of my work, under the supervision of Petros Gebray, mechanical and industrial engineering department, (EIT-M) Mekelle University, Mekelle Ethiopia. Others have not submitted the matter embodied in the thesis for the award of any other degree. All relevant information resources used in the thesis have been duly acknowledged.

Declared by: Ms. Merhawit G/medhin

Signature: 

Date: July 02, 2025GC

Advisor: Petros Gebray Signature:  Date: July 01,2025GC

Acknowledgments

First of all, I want to thank the Almighty God and the Virgin Mary who is at my side and strengthened me throughout my work.

Next, I would like to express my deepest sincere gratitude to my advisor Petros Gebray (PhD candidate) for his unlimited guidance support, encouragement, and excellent supervision that helped me from the selection of this research topic to the end of the thesis, he put in a great deal of effort to shape my work. Without him, it would not have been achievable.

I would like to extend my appreciation to the Moha soft drinks factory for their support in giving ammonia gas.

I also deeply and sincerely thank my brother Michele G/medhin my husband Efrem Kiros, and my family for the unending confidence, constant support, and endless love.

And, finally, I want to thank all those who have contributed to the success of this work one way or the other.

Contents

List of Figures

List of Tables

List of Symbols and Acronyms

L_{st}	The standard meridian for the local time zone
L_{loc}	The longitude of the location
E	Equation of time (in minutes)
n	Day of the year
t_i	Thickness of back collector insulation (m)
t_c	Flat plate collector thickness (m)
k_i	Thermal conductivity of collector insulation $\left(\frac{w}{m^2k}\right)$
T_{pm}	Absorber plate mean temperature (℃)
T_a	Ambient temperature (℃)
A_c	Collector area (m^2)
S	Solar radiation $\left(\frac{w}{m^2}\right)$
U_e	Collector edge heat loss coefficient $\left(\frac{w}{m^2k}\right)$
U_b	Collector bottom heat loss coefficient $\left(\frac{w}{m^2k}\right)$
U_t	Collector top heat loss coefficient $\left(\frac{w}{m^2k}\right)$
U_L	Overall Collector heat loss coefficient $\left(\frac{w}{m^2k}\right)$
L	Length of the collector (m)
w	Width of the collector (m)
$\mathcal{E}_g$	Emittance of glass
$\mathcal{E}_p$	Emittance of the absorber plate
h_w	Wind heat transfer coefficient $\left(\frac{w}{m^{2\circ}\mathrm{C}}\right)$
σ	Stefan-Boltzman constant $\left(\frac{w}{m^2k^4}\right)$
V	Velocity of air $\left(\frac{m}{s}\right)$
N	Number of glass in collector
β	Collector slope (°)
γ	Collector azimuth angle (°)
γ_s	Solar azimuth angle (°)
δ	Thickness (m)
η	Thermal efficiency (-)
θ	Solar incidence angle on the collector (°)
θ_z	Solar zenith angle (°)
σ	Stefan–Boltzmann constant (W m^{-2} K^{-4})
ARS	Absorption Refrigeration System
FPC	Flat Plate Collector

Abstract

Electricity has a vital role in improving the quality of life as it is used in activities such as lighting, heating, air conditioning, refrigeration, transportation, health, communication, entertainment, etc. Lack of electricity can affect the health and agricultural sectors as many of vaccines and agricultural products go to waste to the absence of proper preservation facilities.

To minimize cold preservation problem, a vapor absorption refrigeration system which operates by solar energy was developed, manufactured and experimentally tested. The system used ammonia -water refrigerant absorbent combination. From the cooling load analysis capacity of the system was computed as 55W which is relatively low but enough for the prototype. The system uses 0.39 m^2 area of the flat plate collector and the solar radiation intensity on inclined surface of the location obtained was about 784 W/m^2. The calculated COP of the system was 0.45, with a generator heat input of 120.9 W. This result is favorable when compared to prior studies, which reported COPs in the range of 0.1 to 0.4.

The experimental tests recorded absorber plate and generator temperatures of 100°C and 80°C, respectively. While the generator performance yielded favorable results, further system evaluation was hindered by ammonia leakage. Despite the inability to conduct additional tests due to limited ammonia solution availability, the overall findings indicate with improvements in system sealing and ammonia supply, the proposed system shows promise for rural healthcare and agricultural preservation

Key words: Vapor absorption refrigeration system, solar radiation, cooling load, flat plate collector, Ammonia-water refrigerant, COP

1. INTRODUCTION

In modern society, nearly every aspect of human life relies on electricity, either directly or indirectly. It plays a fundamental role in enhancing quality of life by powering essential activities such as lighting, heating, cooling, refrigeration, transportation, healthcare, communication, and entertainment. Beyond these everyday applications, electricity is a key driver of socio-economic progress. It boosts productivity, improves product quality, reduces dependence on manual labor, and increases efficiency across agricultural and industrial sectors. As a cornerstone of development, electricity enables technological advancements and supports sustainable growth, making it indispensable in today's world. *(Beyene, 2018)*.

With the world's population growing steadily, global energy demand continues to rise. However, access to electricity remains a major challenge, particularly in developing regions. Over one billion people approximately one-seventh of the global population still lack electricity, with 591 million of them residing in Sub-Saharan Africa. Ethiopia reflects this disparity, where only 44.3% of the population had access to electricity as of 2020 (IEA, 2020). This means more than half of Ethiopians remain without power, the majority being rural communities. The lack of reliable electricity hinders economic development, limits education and healthcare access, and perpetuates inequality, underscoring the urgent need for sustainable energy solutions.

The lack of reliable electricity has profound consequences for both healthcare and agriculture. In the healthcare sector, vaccines essential for preventing deadly diseases require consistent refrigeration to maintain efficacy. However, inadequate cold storage leads to significant spoilage, with the World Health Organization estimating that nearly 50% of vaccines are wasted annually in developing nations (Tangka & Kamnang, 2006). This issue is particularly acute in Ethiopia, where around 40% of rural health centers lack electricity access. While some facilities use solar-powered refrigerators and freezers, many remain non-functional due to a shortage of trained cold chain technicians and spare parts, as well as poor maintenance (EFMH, 2015). This gap in reliable refrigeration undermines immunization efforts, leaving vulnerable populations at greater risk of preventable diseases.

Agriculture is the backbone of rural Ethiopia, with most families relying on farming for their livelihoods. However, a critical challenge persists: the lack of proper storage and preservation facilities leads to massive post-harvest losses. Perishable goods such as vegetables, fruits, meat, milk, and fish often spoil before reaching markets due to inadequate refrigeration, poor handling practices, and insufficient processing infrastructure. (*TheBeamMagazine,2019*).

Food preservation plays an essential role in maintaining nutritional value by preventing the degradation of vitamins and minerals, extending shelf life to ensure food remains safe and consumable for longer periods, reducing spoilage and waste, particularly for perishable goods (fruits, vegetables, and dairy), ensuring food quality by preserving taste, texture, and appearance, stabilizing food supply chains, especially in regions with limited access to fresh produce. (*Khurmi and Gupta,2009*).

Furthermore, developing countries face significant barriers to energy distribution due to poor infrastructure, high costs associated with hydroelectric and nuclear power installations, and geographic challenges *(Tangka & Kamnang, 2006).* To address these barriers, there is a growing emphasis on the development of cost-effective, environmentally friendly refrigeration systems powered by low-grade energy sources, including solar, geothermal, and biomass energy *(Dincer & Ratlamwala, 2016).* Ethiopia possesses abundant renewable energy potential including hydro, wind, solar, and bio-energy. But only less than 1% of the wind, geothermal, solar, and less than 10% of the hydro sources are utilized so far. Also, 50% of energy from wood and 30% of energy from agricultural waste have been used *(Beyene, 2018).*

To reduce the challenges in rural healthcare and agriculture, this research focuses on the development of a solar-powered vapor absorption refrigeration system. This system offers a sustainable solution for off-grid applications, providing critical cold storage for vaccines and agricultural products in remote areas. By utilizing solar energy, this refrigeration system can enhance the shelf life of perishable goods and ensure the efficacy of immunization programs, contributing to improved health outcomes and economic resilience. This research aimed to develop a refrigeration system for rural society taking into consideration their economic conditions.

1.1 Background of The Study

Throughout history, humans have developed various methods to preserve food, including drying, salting, and storing ice harvested from frozen lakes. The advent of mechanical refrigeration marked a turning point beginning with Thomas Moore's ice-based refrigerator in 1803 (Wilsdon, 2009) and John Leslie's 1810 absorption refrigeration system, which utilized a water-sulfuric acid solution.

By the 20th century, kerosene-powered refrigerators became a common solution for vaccine storage in off-grid areas. However, their inability to consistently maintain safe temperature ranges highlighted the need for more reliable alternatives.

The 1980s saw the introduction of solar-powered battery refrigerators, which provided a cleaner and more sustainable option for remote regions. Despite their advantages, these systems faced challenges such as high upfront costs and limited battery lifespans (typically 3–5 years), restricting their long-term viability in low-resource settings (WHO & UNICEF, 2015). These limitations underscored the necessity for more affordable, efficient, and durable cooling technologies to meet the needs of underserved populations.

1.2 Problem Statement

Agriculture forms the economic backbone for most rural Ethiopians, yet post-harvest losses remain alarmingly high due to inadequate preservation infrastructure. Perishable commodities including fruits, vegetables, and dairy products frequently spoil before reaching markets, significantly reducing farmers' incomes and exacerbating food insecurity. Simultaneously, the healthcare sector faces parallel challenges. Approximately 50% of vaccines in developing countries become unusable annually due to cold chain failures (Tangka & Kamnang, 2006), with Ethiopia's rural health centers particularly affected.

The energy access disparity compounds these issues: while only 44.3% of Ethiopians have electricity (IEA, 2020), rural areas experience even lower connectivity rates. Notably, 40% of health facilities operate without reliable power (Beyene, 2018), severely compromising vaccine storage capabilities and disease prevention efforts.

This research proposes an innovative solution which is the development of a solar-powered vapor absorption refrigeration system specifically designed for off-grid applications. By harnessing Ethiopia's abundant solar potential (currently less than 1% utilized), the system aims to dramatically reduce post-harvest agricultural losses, ensure proper vaccine preservation in rural health centers, improve overall quality of life through reliable cold storage, and provide sustainable energy solutions for remote communities.

1.3 Objective

1.3.1 General Objective

- To design, construct, and evaluate the performance of a solar-powered vapor absorption refrigeration system for off-grid applications, thereby addressing cold storage challenges in rural Ethiopia.

1.3.2 Specific Objective

- To perform a cooling load analysis for the proposed refrigeration system.
- To design and analyze the components of the absorption refrigeration system.
- To construct a functional prototype of the refrigeration system.
- To test and evaluate the system’s performance.

1.4 Significance of The Study

- Agricultural Preservation: Reducing spoilage of perishable products and improving food security in rural areas.
- Healthcare Support: Ensuring effective cold storage for vaccines, thereby enhancing immunization programs.
- Renewable Energy Utilization: Utilizing Ethiopia’s abundant solar resources to develop a cost-effective, eco-friendly solution.

1.5 Scope and Limitation of The Study

This study focuses on the design, construction, and testing of a solar-powered vapor absorption refrigeration system. The research is constrained by the availability of ammonia as a refrigerant,

which is both reactive with certain metals and costly. The limited availability of small diameter galvanized iron pipes and difficulties in achieving the optimal system diameter also the challenges.

1.6 Thesis Layout

The study structured as follows:

Chapter 1: This introductory chapter includes the background of the study, statement of problem, objectives, scope, significance, and limitations of the study.

Chapter 2: Contains a literature review that relates to the concepts and definition of the absorption system and previous research studies related to solar energy, absorption refrigeration.

Chapter 3: This chapter describes the methodology used to conduct this study. The selection of proper materials for the system is also included in this chapter.

Chapter 4: This chapter includes detailed analysis and design of components. Manufacturing of the components and assembling of the system are also described in this chapter.

Chapter 5: The design and experimental results of the study are discussed in this chapter.

Chapter 6: This chapter contains the conclusion of the study and recommendations.

2. LITERATURE REVIEW

2.1 Introduction

The increasing global demand for sustainable and energy-efficient cooling solutions has driven significant research into solar-powered refrigeration systems. Among these, solar absorption refrigeration systems (SARS) have emerged as a promising alternative to conventional vapor compression systems, particularly in off-grid and rural areas where electricity access is limited. These systems utilize solar thermal energy to drive the refrigeration cycle.

This literature review examines the fundamental principles, components, and performance of solar absorption refrigeration systems, focusing on solar energy availability and radiation dynamics, solar thermal collectors, absorption refrigeration technology and previous research.

The review synthesizes findings from various studies to identify gaps, challenges, and opportunities for improving system efficiency, cost-effectiveness, and scalability. By analyzing existing literature, this section provides a foundation for understanding the design and operational considerations of solar absorption refrigeration systems, particularly for applications such as food preservation and vaccine storage in remote regions.

The discussion begins with an overview of solar radiation and collector technologies, followed by an in-depth analysis of absorption refrigeration principles and comparative studies on system performance. Finally, key findings from previous research are summarized to highlight trends, limitations, and future research directions.

2.2 Solar System

According to (*John and William,1980*), the sun has an effective black body temperature of 5777k. In the central interior region, the temperature reaches $8x10^6$ to $40x10^6$k, and the density is about 100 times that of water. Then this energy in the interior region transfers to the outer surface and radiates to space. The solar constant which is the mean radiative flux density outside of the earth's atmosphere is constant Gsc 1367W/m^2.

All the radiation from the sun doesn't reach the earth's surface. Some of that is absorbed and scattered by the atmosphere. The radiation reaches the earth in two components namely beam radiation and diffuse radiation. Beam radiation is the solar radiation received on the earth's surface

without being scattered by the atmosphere and diffuse radiation is the solar radiation received on the earth's surface after it is scattered by the atmosphere. The amount of solar radiation that reaches the earth's surface differs from place to place due to time of day, geographic location, season, the local landscape, and weather.

2.2.1 Direction of Beam Radiation

The geometric relationships between a plane of any particular orientation relative to the earth at any time and the incoming beam solar radiation, that is, the position of the sun relative to that plane, can be described in terms of several angles. These angles are:

Latitude (Φ): the angular location north or south of the equator, north positive; $-90^{O} \leq \Phi \leq 90^{O}$ (13.494^{O} for Mekelle)

Declination (δ): the angular position of the sun at solar noon (i.e., when the sun is on the local meridian) concerning the plane of the equator, north positive; $-23.45^{O} \leq \delta \leq 23.45^{O}$

Slope (β): the angle between the plane of the surface in question and the horizontal; $0^{O} \leq \beta \leq 180^{O}$ ($\beta > 90^{O}$ means that the surface has a downward-facing component)

Surface azimuth angle (Υ): the deviation of the projection on a horizontal plane of the normal to the surface from the local meridian, with zero due to south, east negative, and west positive; $-180^{O} \leq \Upsilon \leq 180^{O}$

Hour angle (ω): the angular displacement of the sun east or west of the local meridian due to rotation of the earth on its axis at 15^{O} per hour; morning negative, afternoon positive.

The angle of incidence (θ): the angle between the beam radiation on a surface and the normal to that surface.

Zenith angle (θz): the angle between the vertical and the line to the sun, i.e., the angle of incidence of beam radiation on a horizontal surface.

Solar attitude angle ($\alpha_{s)}$): the angle between the horizontal and the line to the sun, i.e., the complement of the zenith angle.

Solar azimuth angle (Υs): the angular displacement from the south of the projection of beam radiation on the horizontal plane. Displacements east of south are negative and west of south are positive.

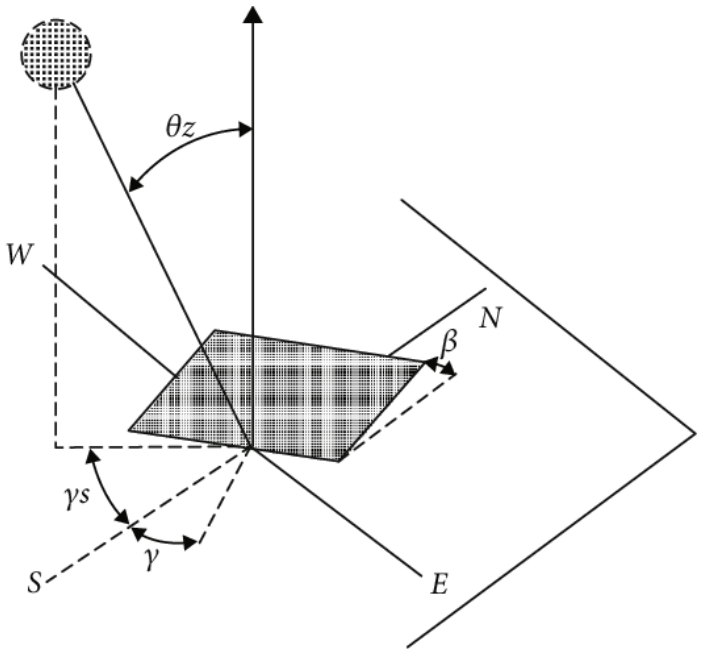

Figure 2. 1: Solar radiation angles(Laveyne et al., 2020)

*Table 2. 1: Recommended Average Days for Months and Values of N by Months (*John and William,1980*)*

Month	n for ith Day of Month	For the Average Day of the Month		
		Day	n, of the year	δ, Declination
January	i	17	17	-20.9
February	31+i	16	47	-13.0
March	59+i	16	75	-2.4
April	90+i	15	105	9.4
May	120+i	15	135	18.8
June	151+i	11	162	23.1
July	181+i	17	198	21.2
August	212+i	16	228	13.5
September	243+i	15	258	2.2
October	273+i	15	288	-9.6
November	304+i	14	318	-18.9
December	334+i	10	344	-23.0

2.3 Solar Thermal Collectors

Solar thermal collectors are devices that capture solar radiation and convert it into usable thermal energy. They achieve this by transferring absorbed heat to a working fluid, such as water, oil, or air. Solar collectors are broadly categorized into two types (*John and William,1980*).

Non-concentrating collectors: These include flat plate and evacuated tube collectors, which are commonly used for low to medium temperature applications.

Concentrating collectors: These systems use reflectors or lenses to focus solar radiation onto a small area, enabling higher operating temperatures.

Table 2. 2: Types of Solar Thermal Collectors and Their Typical Temperature Range (Goswami et all., 2000)

Type of Collector	Concentration Ratio	Typical Working Temperature Range (°C)
Flat-plate collector	1	≤70
High-efficiency flat-plate collector	1	60–120
Fixed concentrator	3–5	100–150
Parabolic trough collector	10–50	150–350
Parabolic dish collector	200–500	250–700
Central receiver	500 to >3000	500 to >1000

2.3.1 Flat Plate Collectors

Flat plate collectors are widely used due to their simplicity, low cost, and reliability. They are typically used for applications requiring temperatures between 40°C and 80°C. A flat plate collector consists of the following components:

Absorber plate: Captures solar radiation and transfers heat to the working fluid.

Transparent cover (glass): Minimizes heat loss while allowing solar radiation to pass through.

Insulation: Reduces heat losses from the back and sides of the collector.

Casing: Provides structural support and protection.

The basic flat plate collector energy balance equation is:

$$Qu = Ac[S - U_L (Tpm - Ta)] \quad (2.1)$$

Where:
Qu = Useful energy output of a collector
Ac = Collector area
S = Absorbed solar radiation per unit area
U_L = Collector overall heat loss coefficient
Tpm = Mean absorber plate temperature
Ta = Ambient temperature

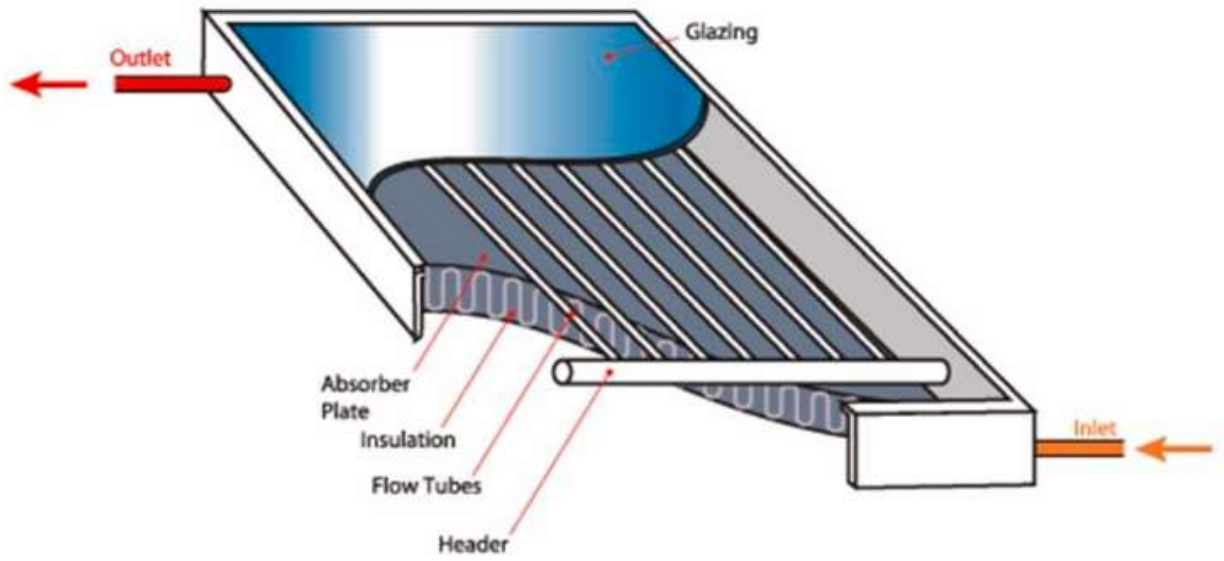

Figure 2. 2: Flat plate collector(Shirazi et al., 2018)

To model flat plate collectors some simplifying assumptions have been made by (*John and William,1980*)

1. Performance is a steady state.
2. Construction is of sheet and parallel tube type.
3. The headers cover a small area of the collector and can be neglected.
4. The headers provide uniform flow to tubes.
5. There is no absorption of solar energy by a cover insofar as it affects losses from the collector.
6. Heat flow through a cover is one-dimensional.
7. There is a negligible temperature drop through a cover.

8. The covers are opaque to infrared radiation.
9. There is a one-dimensional heat flow through back insulation.
10. The sky can be considered as a black body for a long wavelength radiation at an equivalent sky temperature.
11. Temperature gradients around tubes can be neglected.
12. The temperature gradient in the direction of flow and between the tubes can be treated independently.
13. Properties are independent of temperature.
14. Loss through front and back are to the same ambient temperature.
15. Dust and dirt on the collector are negligible.
16. The shading of the collector absorber plate is negligible.

2.4 Refrigeration system

Refrigeration involves transferring heat from a low-temperature source to a high-temperature sink, maintaining the source temperature below ambient conditions. Refrigeration systems are widely used across industries, including food preservation, pharmaceuticals, and air conditioning (Wang, 2000).

2.4.1 Absorption Refrigeration System

The vapor absorption refrigeration system (ARS) is powered by thermal energy, making it suitable for applications where low-grade heat sources like solar energy are available. The basic working principle involves:

Evaporation: The refrigerant absorbs heat and evaporates, producing a cooling effect.

Absorption: The refrigerant vapor is absorbed into a solution (e.g., ammonia into water).

Regeneration: The solution is heated, releasing refrigerant vapor, which is condensed to liquid form.

The ammonia-water (NH_3-H_2O) system is commonly used for low-temperature refrigeration.

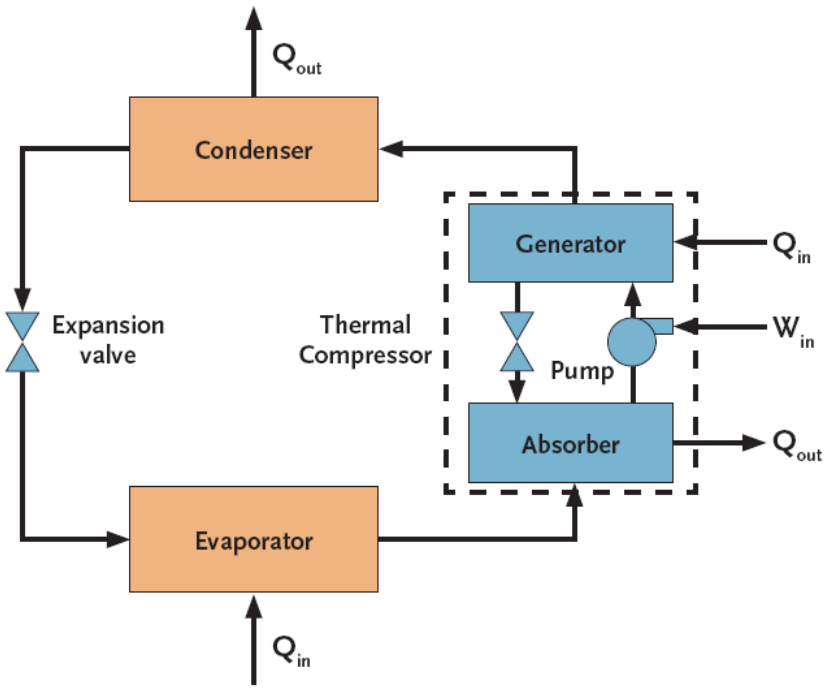

Figure 2. 3: Vapor absorption refrigeration system(CIBSE Journal,2009)

.

ARSs for industrial and domestic applications have been attracting increasing interest throughout the world because of the following advantages over other refrigeration systems (Dinçer, 2003).

- Quiet operation with minimal mechanical wear.
- Efficient utilization of renewable energy sources.
- Reliable performance under variable load conditions.

2.4.2 Vapor Compression System

In contrast to ARS, vapor compression systems use mechanical energy to compress and circulate refrigerant. These systems rely heavily on electricity, limiting their feasibility in off-grid applications.

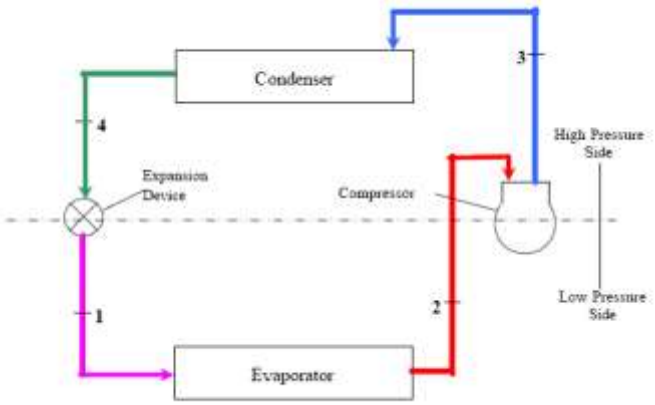

*Figure 2. 4: Vapor compression system(*EnggCyclopedia*, 2012)*

2.4.3 Other Refrigeration Systems

- Air or gas expansion systems: In this system, gas is compressed to a high pressure by mechanical energy. It is then cooled and expanded to a low pressure. Because the temperature of air or gas drops during expansion, a refrigeration effect is produced.
- Steam Jet Refrigeration System: This system uses the principle of boiling water below 100°C.
- Thermoelectric Refrigeration Systems: The passage of an electric current through junctions of dissimilar metals causes a fall in temperature at one junction and a rise at the other, the Peltier effect. Applications are limited in size, owing to the high electric currents required, and practical uses are small cooling systems for military, aerospace, and laboratory use.
- Magnetic Refrigeration: Magnetic refrigeration depends on what is known as the magnetocaloric effect, which is the temperature change observed when certain magnetic materials are exposed to a change in magnetic field *(Sachin, 2020)*.
- Adsorption Cooling System: The adsorption process is a surface phenomenon in which a solid porous surface with a large surface area and adsorptive capacity acts as a primary component of the system. The combination of working fluids used in the adsorption systems greatly affects the performance of the system. Working fluids used by different researchers are silica gel–water, activated-carbon–methanol, activated-carbon–ammonia, zeolite–water, activated-carbon–granular, and fiber adsorbent. A standard adsorption

system consists of an adsorbent bed, an evaporator, and a condenser *(Dincer & Ratlamwala, 2016)*.

Table 2. 3: Coefficient of performance of different cooling systems (Dincer & Ratlamwala, 2016)

No_	Cooling system	Cop
1	Solar PV cooling	0.7
2	Solar thermoelectric	0.3-0.5
3	Thermo- mechanical	0.49
4	Desiccant	0.35-0.94
5	Adsorption	0.05-0.3
6	Single effect absorption	0.5-0.7
7	Double effect absorption	0.8-1.2
8	Triple effect absorption	1.4-2
9	Quadruple effect absorption	1.7-2.5

However, among all the different renewable energy-based cooling technologies explained above, absorption refrigeration systems provide better coefficient of performance and operating temperature ranges. These benefits make absorption refrigeration systems an ideal replacement for conventional cooling systems *(Dincer & Ratlamwala, 2016)*.

The advantages of a vapor absorption refrigeration system over a vapor compression refrigeration system are summarized in table 2.4: *(Khurmi and Gupta,2009)*

Table 2. 4: Comparisons of vapor absorption and vapor compression refrigeration system

Feature	Vapor Absorption Refrigeration (VAR)	Vapor Compression Refrigeration (VCR)
Driving Force	Heat Energy	Mechanical Energy
Primary Moving Part	Pump	Compressor
Noise Level	Quieter	Louder
Wear and Tear	Less	More
Load Variation Handling	Better performance at varying loads	Poor performance at partial loads
Low Evaporator Pressure Operation	Can operate at lower pressures with minimal capacity reduction	Capacity drops significantly
Liquid Refrigerant Impact	Minimal impact	Requires superheated vapor to prevent compressor damage
Scalability	Can be built in much larger capacities	Limited by the size of single compressor units

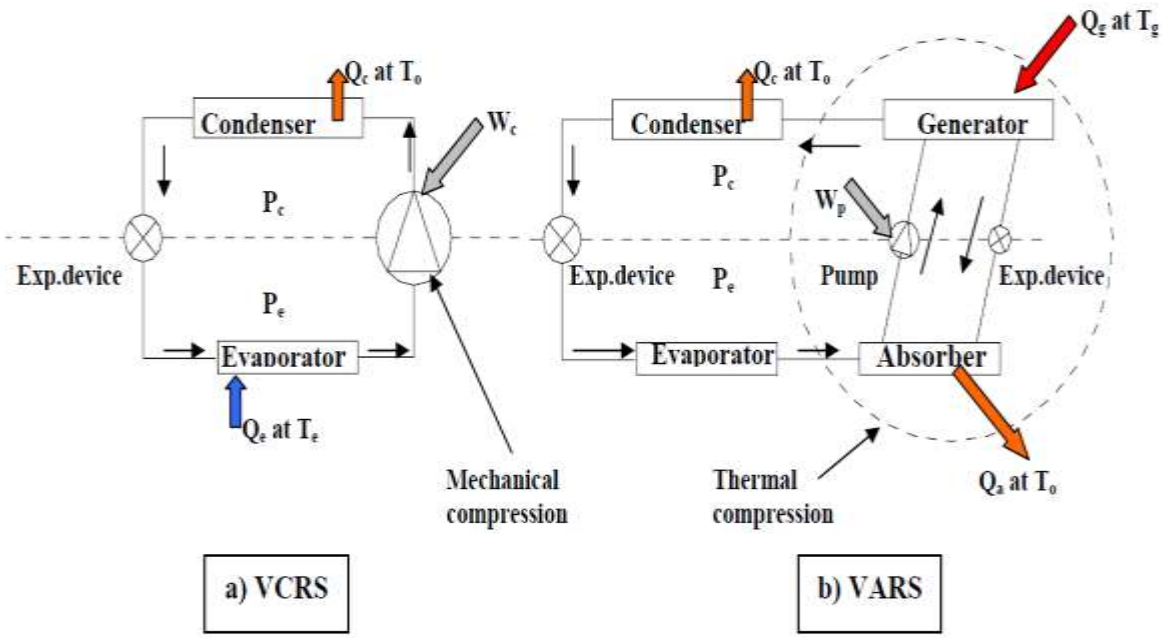

*Figure 2. 6: Basic vapor compression and vapor absorption refrigeration system(*IIT, Kharagpur,2008*)*

2.5 Refrigerant - Absorbent Combinations

The performance of absorption refrigeration systems is highly dependent on the refrigerant-absorbent pair. Common pairs include:

The most commonly used refrigerant-absorbent pairs in commercial systems are:(*John and William,1980*)

- Water-Lithium Bromide (H_2O-LiBr) system for above 0^oC applications such as air conditioning due to the crystallization of water. Here water and lithium bromide are refrigerant and absorbent respectively.
- Ammonia – Water (NH_3 – H_2O): Suitable system for applications with ammonia as refrigerant and water as absorbent.

Currently, large water-lithium bromide systems are extensively used in air-conditioning applications, whereas large ammonia-water systems are used in refrigeration applications.

Although ammonia is toxic and flammable due to its availability and achieving low cabinet temperature ammonia water mixture is used as a refrigerant absorbent combination.

2.5.1 Criteria for Selection of Refrigerants

In the selection of an appropriate refrigerant for use in a refrigeration system, there are many criteria to be considered. Briefly, the refrigerants are expected to meet the following conditions according to *(Dincer, 2003)*:

- Ozone and environment-friendly
- Low boiling temperature
- Low volume of flow rate per unit capacity
- Vaporization pressure lower than atmospheric pressure
- The high heat of vaporization
- Non-flammable and nonexclusive
- Noncorrosive and nontoxic
- Nonreactive and no depletive with the lubricating oils of the compressor
- Nonacidic in case of a mixture with water or air
- Chemically stable
- Suitable thermal and physical properties (e.g., thermal conductivity, viscosity)
- Commercially available
- Easily detectable in case of leakage, and
- Low cost

2.6 Previous Works

Several studies have explored the feasibility, design, and performance of solar-powered absorption refrigeration systems (ARS) to address energy challenges in off-grid and rural areas. These studies provide valuable insights into system design, operational performance, working fluid selection, and limitations. This section discusses key contributions and findings from relevant works.

An intermittent ammonia-water absorption refrigeration system powered by solar energy was designed, constructed, and tested *(Mondal et al.,2015)*. The system utilized a parabolic solar collector as the heat source to generate ammonia vapor from a calcium chloride-ammonia solution. The system Components are a generator for heating the solution, a condenser to liquefy ammonia vapor, a storage tank for liquid ammonia, and an evaporator for producing the cooling effect.

Operational. The generator temperature reached 105°C with an average solar generation time of 6–7 hours. The evaporator achieved a minimum temperature of 8.5°C, while the system's COP (Coefficient of Performance) ranged between 0.104 and 0.126, with an average of 0.118. Here the cooling capacity and COP decreased when the generator temperature dropped due to insufficient solar input. Moreover, the ammonia storage tank temperature fluctuated, reducing the system's cooling effect. This study demonstrated the technical feasibility of using intermittent solar heat for ammonia-water ARS, highlighting the importance of maintaining stable generator temperatures to ensure consistent performance.

Tangka and Kamnang developed and tested a simple solar-powered ARS using ammonia-water as the refrigerant-absorbent pair*(Tangka & Kamnang, 2006)*.The system aimed to achieve refrigeration for vaccine and food preservation in rural areas. The solar collector temperature achieved a maximum of 100°C. The lowest temperature recorded in the refrigeration compartment was 4°C, sufficient for vaccine storage. The system's COP was calculated to be 0.487. Covering the collector at the end of the generation cycle was found critical to preventing additional heat gain. Ambient heat gain caused challenges in maintaining the refrigeration temperature throughout the day. This study demonstrated the potential of ammonia-water systems for achieving temperatures suitable for vaccine preservation. However, it emphasized the need for proper insulation and system optimization to prevent thermal losses.

Kim and Ferreira *(Kim & Infante Ferreira, 2008)* conducted a comprehensive review of solar-powered refrigeration technologies, including: Solar electric systems (photovoltaic-driven compressors). Solar thermal systems such as absorption, adsorption, and thermo-mechanical refrigeration systems. The study compared these technologies based on energy efficiency and economic feasibility. Absorption systems demonstrated superior energy efficiency when powered by low-grade heat sources, such as solar thermal energy. Adsorption systems, while effective, were bulkier and more expensive than absorption chillers. Solar PV cooling systems were found to be the least cost-effective due to high system costs and energy losses. Single-effect absorption systems emerged as the most economical and practical solution for solar-powered cooling. For higher temperatures and larger applications, double-effect absorption systems offered improved COP values. This review stares that absorption refrigeration systems are ideal for harnessing solar thermal energy in off-grid, providing both energy efficiency and cost-effectiveness.

Different solar refrigeration and cooling methods was reviewed in detail by Sarbu and Sebarchievici *(Sarbu & Sebarchievici, 2013)*. Based on the coefficient of performance (COP), the absorption systems are preferred over the adsorption systems, and higher temperature issues can be achieved with solar adsorption systems. Also, the adsorption cooling typically needs lower heat source temperatures than the absorption cooling. In comparing a liquid desiccant system with a solid desiccant system liquid desiccant system has a higher thermal coefficient of performance. The thermodynamic properties of most common working fluids, as well as the use of ternary mixtures in solar-powered absorption systems, have been reviewed in the paper. The ejector system represents thermo-mechanical cooling and has a higher thermal COP but requires a higher heat source temperature than other systems.

Osman and Yanling *(Mohammed & Yanling, 2017)*analyzed a single-stage ammonia-water absorption refrigeration system to reduce its driving temperature, thereby lowering the cost of solar collectors. The study focused on incorporating an effective solution heat exchanger (SHX) to improve energy recovery. The driving temperature was reduced to 90°C using a heat exchanger with 80% effectiveness. The system achieved a significant improvement in COP and exergy efficiency. By reducing the driving temperature, the study demonstrated that less expensive solar collectors could be used, making ARS systems more accessible and affordable for off-grid applications. This work states the importance of optimizing system components to lower the operational costs and improve the economic feasibility of solar absorption systems.

Siddiqui and Said *(Siddiqui & Said, 2015)* presented a review of different published works in the field of solar-powered absorption systems that utilize pairs of working fluids. Solar-powered absorption refrigeration systems, diffusion absorption systems, ejector-based absorption systems, compression absorption systems, and cogeneration/trigeneration absorption systems were reviewed. The thermodynamic properties of most common working fluids as well as the use of ternary mixtures in solar-powered absorption systems have been reviewed in this study. The review indicates that along with aqua-ammonia and LiBr–water, certain other working fluids have theoretically shown good performance such as lithium nitrate–ammonia, sodium thiocyanate–ammonia, TFE–TEGDME, methanol–TEDGME, monomethylamine–water and LiCl–water. It is also found that, for diffusion absorption systems, the TFE–TEGDME working pair has

theoretically shown good performance. The review also indicates that the ternary mixture of LiBr-CHO2K–water has shown good performance compared to other ternary mixtures.

Prof. Dr. Adel A. Al-Hemiri and Ahmed Deaa Nasiaf *(A. Al-Hemiri & Deaa Nasiaf, 2010*) studied the coefficient of performance for solar absorption refrigeration by using direct solar energy. The ammonia–water mixture was used as a refrigerant–absorbent combination and the fraction of aqueous ammonia was 0.45. The experiments were carried out in a solar absorption system. The system was constructed with different components solar collector generator (0.25 m × 0.25 m × 0.04m), a water-cooled condenser, a liquid receiver that receives liquid from the condenser, and an evaporator. The maximum generator temperature achieved was 92° - 97° and the minimum evaporator temperature was 5°C - 10°C. The coefficient of performance ranged from 0.1096 - 0. 2396. In the study, it was seen that the coefficient of performance, cooling ratio, and amount of cooling obtainable increased with increasing maximum generator temperature and pressure. While the minimum evaporator temperature and concentration decreased with increasing maximum generator temperature and pressure.

An intermittent solar absorption refrigeration system was designed and fabricated by *(Shahad & Hamzah, 2015)*. The maximum pressure and temperature achieved in the generator were found to be 12 bar and 120^{o}C respectively using a 2 m^2 parabolic trough concentrator (PTC). The system was tested using different concentrations (25%, 30%, 35%, and 40%) of ammonia water solution. As the concentration of the solution increased the amount of ammonia vapor produced was increased. More than 120 tests were done in one year to evaluate the system experimentally. The coefficient of performance depends on concentration as well as the pressure achieved in the unit. In the study, five main parameters were used to evaluate the performance of the experimental system namely the amount of ammonia produced in the generator, the insolation, the solar radiation incident on the CPC, the cooling capacity, and the solar coefficient of performance. The coefficient of performance was in the range of 0.01-0.09.

Dara J. et al. *(Dara et al., 2013)* presented the evaluation of the performance of a passive flat plate solar collector. The research investigated the variations of top loss heat transfer coefficient with absorber plate emittance; and air gap spacing between the absorber plate and the cover plate. The effects of these parameters on the performance of the solar collector were also investigated. It can be seen that an increase in the air gap spacing resulted in to decrease in the top loss heat transfer coefficient, but the effect of air gap spacing becomes less significant with air gap spacing of above

33mm. It was observed that high plate emittance tends to dissipate more heat to the atmosphere and consequently resulted in to increase in top loss heat transfer coefficient which led to reduced system performance. Also, it was observed that an increase in air gap spacing between the absorber plate and the cover plate resulted in a decrease in the top loss heat transfer coefficient. A passive flat-plate solar collector was observed to perform better at a lower mean plate temperature.

Ammonia-water systems are effective for refrigeration in off-grid areas due to their ability to achieve low temperatures. Solar thermal collectors, particularly flat plate and parabolic trough collectors, are widely used as heat sources for absorption systems. Optimizing system components, such as the generator and heat exchangers, significantly improves performance and reduces operational costs. Major challenges include maintaining stable generator temperatures, preventing refrigerant leakage, and ensuring proper insulation. By addressing the limitations identified in previous works, this research aims to develop an efficient, cost-effective, and reliable solution for food and vaccine preservation.

3. METHODOLOGY and MATERIAL SELECTION

3.1 Introduction

The design and performance of a solar-powered absorption refrigeration system depend on careful selection of materials, components, and system configurations. This section outlines the methodology used to develop the system, including design considerations and material selection criteria.

3.2 Methodology

A schematic representation of the methodology is shown in Figure 3.1.

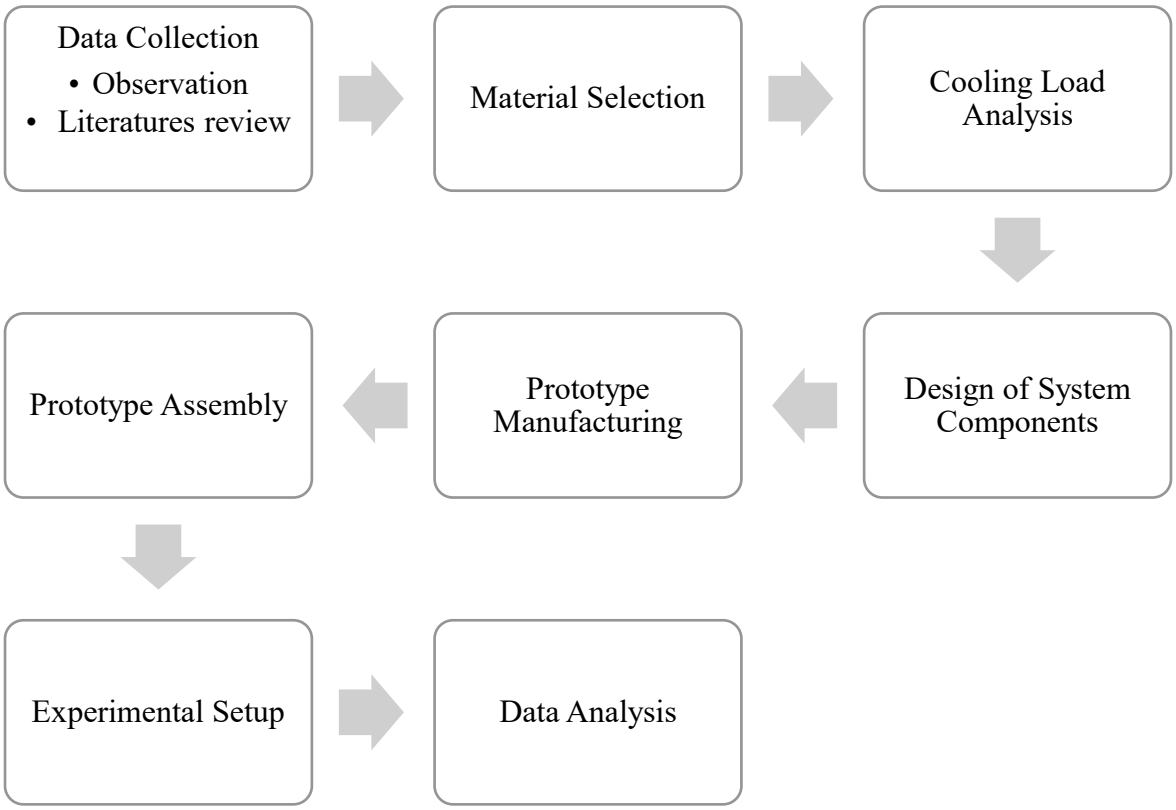

Figure 3. 1: Methodology of the study

The overall methodology is summarized as below:

Literature Review: A detail investigation of solar thermal systems, refrigeration technologies, and previous works was conducted to identify gaps and some design considerations.

Cooling Load Analysis: The total refrigeration capacity required for the system was calculated using heat transfer equations.

Design of System Components: Major components, including the flat plate collector, condenser, evaporator, absorber, generator, and capillary tube, were designed based on thermodynamic principles and performance requirements.

Material Selection: Materials for each component were chosen based on thermal, mechanical, and chemical compatibility with the working fluid (ammonia-water).

Prototype Construction: The designed system was manufactured, assembled.

Experimental Setup: The prototype was tested under solar radiation conditions to measure performance parameters, including temperature, pressure.

Data Analysis: Experimental results were compared with theoretical predictions to evaluate system performance.

3.3 Material Selection

Material selection is a critical aspect of the system's design to ensure efficiency, durability, and cost-effectiveness. Each component was carefully evaluated based on factors such as thermal conductivity, corrosion resistance, strength, and compatibility with the ammonia-water working pair.

3.3.1 Flat Plate Collector

The flat plate collector (referring figure 2.2) serves as the heat source, converting solar energy into thermal energy to drive the generator. It is designed based on two principles: A black-painted absorber plate to maximize solar energy absorption and a glass cover to trap heat within the collector. The selected materials and their justifications are as follows:

I. **Absorber plate**:

The collector absorber plate should have high thermal conductivity, adequate tensile and comprehensive strength, and good corrosion resistance. Metals like copper, aluminum, and stainless steel are mostly used as absorber plates.

Table 3. 1: Comparison of absorber plates with different materials

(Source: https://www.engineeringtoolbox.com)

Criteria's	Aluminum	Copper	Steel
Density(kg/m^3)	2712	8940	7850
Melting point (°C)	660	1084	1510
Weight	Less	More	Medium
Emissivity	0.09	0.052	0.075
Strength (MPa)	Less	Medium	More
Thermal conductivity(W/mK)	237	413	54
Resistance to corrosion	High	Medium	Low
Cost	Medium	More	Less

Based on the comparison in the table aluminum absorber was selected and it is painted with black to increase its absorptance to solar radiation.

II. **Cover glass**:

The most critical factors for the cover plate materials are strength, durability, non-degradability, and solar energy transmission. Therefore, tempered glass of thickness 6 mm is used as a covering material because of its proven durability and because it is not affected by ultraviolet radiation from the sun.

III. **Casing**:

Iron sheet is selected for the casing material. Iron is cost-effective and structurally strong, providing good support for the flat plate collector.

IV. **Insulation:**

A layer of insulating material can reduce heat losses from the back and edge of an absorber plate and should be able to withstand the collector stagnation temperatures. Fiberglass is selected for the back and edge of absorber plate insulation because it presents no fire hazards compared to

other polymeric foams and can resist the high collector stagnation temperature. The main function of the insulator is to minimize heat lost from the bottom and sides of the casing of FPC. To prevent heat loss in the flat plat collector the back and sides of the collector are insulated using fiberglass.

V. **Sealant**:

Sealing materials are applied to ensure the solar collector is not affected by weather conditions. Silicon is used as a sealing. In addition, a gasket maker and Epoxy are used to prevent leakage through connections of valves and thermocouples.

3.3.2 Refrigerator Compartment

An aluminum composite panel which consists of two thin coil-coated aluminum sheets bonded to a core is selected for the body of the cabinet. The panel has good insulation properties and quality with 0.024-0.05 $\frac{W}{mk}$ thermal resistance. Since ammonia has good thermal conductivity for the part between the evaporator and the internal part of the cabinet aluminum sheet of thickness 1mm is selected which accumulates heat transfer between the evaporator and the products which going to be cooled. For the door of the cabinet aluminum frame and thick plastic are selected. To connect the pieces of the cabinet different sizes of bolts are selected.

The choice of insulation is very important as it accounts for a large proportion of the total construction cost. The insulation material and thickness are also important from an energy point of view. A thermos-cool insulation (thermal conductivity 0.033 to 0.038 W/mk) with 5mm thickness is used between the inner and outer walls of the cabinet so that heat loose through the cabinet wall will decrease.

3.3.3 Condenser

The condenser is a heat - exchanger used to condense the ammonia vapor to its liquid state. In the condenser, heat is extracted from the refrigerant at constant pressure. As heat transfers from the refrigerant inside the pipe to the air outside the pipe the refrigerant condenses to liquid and is collected at the bottom of the condenser before proceeding to the capillary tube. Ammonia will quickly corrode copper, aluminum, zinc, and all alloys of these metals, therefore these metals cannot be used where ammonia is present. Instead, steel, cast iron, stainless steel, and some plastics can be used in ammonia absorption refrigeration systems. For condenser pipes galvanized iron is

selected due to its chemically compatible with ammonia, cost-effective, and readily available. Since air cooled condenser is used 1mm aluminum fins are selected to accumulate heat transfer.

3.3.4 Evaporator

The refrigerant at very low pressure and temperature from the capillary tube enters the evaporator and produces the cooling effect. For evaporator pipes galvanized iron is selected due to its cost and availability.

3.3.5 Absorber

The ammonia vapor from the evaporator absorbs into the solution in the absorber. For the absorber galvanized iron pipe is selected.

3.3.6 Separator

During regeneration not only ammonia vapor goes to the condenser some water vapor is carried out with ammonia. To prevent water from entering the condenser separator will be installed between the generator and the condenser. For the separator, a 4mm thick galvanized iron pipe is selected.

3.4 Materials for Solution Preparation

The working fluid for the system is a 40% ammonia-water solution. In the preparation process components including scale, volume-measuring flask, plastic bottles, aluminum foil, and cold water was used. Fig 3.2 illustrates the equipment setup used for solution preparation.

Figure 3. 2: Equipment used to prepare ammonia solution

4. DESIGN ANALYSIS

4.1 Introduction

This chapter provides a comprehensive design analysis of the solar-powered vapor absorption refrigeration system. It includes detailed calculations, numerical values, and thermodynamic analysis for each component, ensuring that the design meets performance requirements.

4.2 Cooling Load Analysis

The total cooling load is the sum of all heat gains into the refrigeration compartment, including heat transfer through the walls, cooling the stored products, respiration heat, and heat gain due to door openings. A 10% safety factor is added to account for uncertainties.

The assumption was made to simplify the calculations which were:

- All six walls of the cabinet had the same thickness
- All the cabinet walls had the same heat transfer characteristics
- The internal temperature of the cabinet is uniform at 3°C
- The ambient temperature is 24°C
- Heat transfer resistance through metal cases was neglected
- Radiation exchange at the inner surface was neglected

4.2.1 Environmental Heat Gains

Heat transfer to the cabinet takes place through all three mechanisms i.e. conduction, convection, and radiation. The internal and external surfaces are characterized by heat transfer coefficients hi and ho, respectively, and the insulation by its thermal conductivity k.

The heat transfer that takes place from the external to the internal surfaces is conducted across the insulation through a varying area. Thus, the conduction area is taken as the mean of internal and external areas. Therefore,

Table 4.1: Compartment dimensions

Name	Dimension
Width of cabinet	0.5m
Length of cabinet	0.4m
Height of cabinet	0.5m

Wall thickness	0.05m
Internal surface area (Ai)	$0.8m^2$
External surface area (Ao)	$1.3m^2$
Mean conduction area (Am)	$1.035m^2$
Internal cabinet volume (V)	$0.048m^3$ = 48Liter

Let's assume that the cabinet is always placed in some sheltered place. Thus, the system is analyzed assuming heat gains through natural convection. There are four vertical and two horizontal faces of the cabinet.

The overall heat transfer across the cabinet walls was then calculated by the equation *(ASHRAC, 2010).*

$$UA = \left[\left(\frac{1}{hiAi}\right) + \left(\frac{t}{kAm}\right) + \left(\frac{1}{hoAo}\right)\right]^{-1} \qquad (4.1)$$

Using K= 0.0355 $\frac{W}{mk}$and hi=5, ho=25$\frac{W}{m2k}$

$$UA = 0.6\frac{W}{K}$$

$$Q_g = UA\,(To - Ti) \qquad (4.2)$$

$$Q_g = 16.5\,W$$

4.2.2 Cooling Load of Product

This is heat that must be removed to bring products to storage temperature. Let's take the specific heat and density of the product as equal to water which is 4.18 $\frac{kJ}{kg}.K$ and 1000 $\frac{kg}{m3}$ respectively. Then, the product cooling load assuming 1.25 liter of the total volume occupied by the product be:

$$Q_{pr} = \rho V Cp \Delta T \qquad (4.3)$$

$$Q_{pr} = 1 \times 1.25 \times 4180 \times \frac{(24 - 3)}{1hr \times 3600}$$

$$Q_{pr} = 30.47\,W$$

4.2.3 Respiration Load

The product respiration heat is the heat generated by living products such as fruits and vegetables in storage. For tomato $hres$=8881.8 KJ/kg

$$Qre = \frac{m * hres}{1hr * 3600} \qquad (4.4)$$

$$Qre = 3.08\ W$$

4.2.4 Cooling Load Due to Intermittent Door Opening

When the refrigerator door is opened some of the cold air inside the cabinet is replaced with the outside air which is warm and humid. Assuming the door is opened every hour. Half the cold is replaced by warm saturated air every time the door is opened and the warm air is cooled to 3ºC in half an hour, the cooling load would be calculated as follows.

The volume of air inside the refrigerator = 18 L

Volume of warm saturated air = 0.5 x 18 = 9 L

Moisture contents of saturated air at 24^0C = 0.042 g/ 1

Latent heat of condensation of water = 2250 J/g

Neglecting the heat contents of air compared to water the cooling load due to the warm moist air entering the compartment would be:

$$Qair = 9\ x\ 0.042\ x \frac{(2250 + 4.18\ x\ 18)}{30 * 60} \qquad (4.5)$$

$$Qair = 0.488\ W$$

4.2.5 Total Cooling Capacity

The total cooling capacity of the refrigerator would be the sum of all the cooling loads and 10% of the safety factor

$$Qt = 55\ W$$

4.3 Design of the Absorption Refrigerator Components

4.3.1 Design Analysis of Flat Plate Collector

4.3.1.1 Solar Time(t)

We need to convert the standard time to solar time in doing solar calculations. Solar time is the time based on the apparent angular motion of the sun across the sky, with solar noon the time the sun crosses the meridian of the observer *(John and William,1980).*

$$Solar\ time\ =\ Standard\ time\ +\ \frac{[4(L_{st}-L_{loc})+E]}{60} \qquad (4.6)$$

Where: -

Standard time = local clock time (Assume 9:00A.M)

Lst = the standard meridian for the local time zone (315^{o} W for Ethiopia)

$Lloc$ = the longitude of the location in question (320.53^{o} W for Mekelle)

E = equation of time (in minutes)

$$E\ =\ 229.2\ (0.000075\ +\ 0.001868\ Cos\ B\ -\ 0.032077\ Sin\ B\ -\ 0.014615\ Cos\ 2B\ -\ 0.04089\ Sin\ 2B) \qquad (4.7)$$

$$B\ =\ (n-1)\frac{360}{365} \qquad (4.8)$$

n = day of the year. From Table 2.1 for January 29, n = 29

$$B\ =\ 27.616^{o}$$

$$E\ =\ -12.6205\ minutes$$

$$Solar\ time\ (t)\ =\ 8{:}25\ A.M$$

4.3.1.2 Direction of Beam Radiation

The geometric relationships between a plane of any particular orientation relative to the earth at any time and the incoming beam solar radiation, that is, the position of the sun relative to that plane, can be described in terms of several angles (*John and William,1980*)These angles are:

Latitude (Φ): The angular location north or south of the equator, north positive; $-90^{O} \leq \Phi \leq 90^{O}$ (13.494^{O} for Mekelle)

Declination (δ): The angular position of the sun at solar noon (i.e. when the sun is on the local meridian) concerning the plane of the equator, north positive; $-23.45^{O} \leq \delta \leq 23.45^{O}$, and given by

$$\delta = 23.45 * \text{Sin}\left(\frac{360(284+n)}{365}\right) \qquad (4.9)$$

$$\delta = -18.298^{O}$$

Slope (β): The angle between the plane of the surface in question and the horizontal; $0^{O} \leq \beta \leq 180^{O}$ ($\beta > 90^{O}$ means that the surface has a downward-facing component)

If the latitude is below 25^{O}, we use the latitude times 0.87 to find the best angle from the horizontal at which the panel should be tilted.

Latitude of Mekelle is 13.494^{O}N, therefore $\beta = 11.74^{O}$ N

Surface azimuth angle (ϒ): The deviation of the projection on a horizontal plane of the normal to the surface from the local meridian, with zero due to south, east negative, and west positive; $-180^{O} \leq \Upsilon \leq 180^{O}$

In the northern hemisphere between the latitude of 23 and 90, the sun is always in the south. Therefore, the modules on an array are directed to the south to get the most out of the sun's energy (*Greentech Renewables*, 2010).

Therefore $\Upsilon = 0^{O}$

Hour angle (ω): The angular displacement of the sun east or west of the local meridian due to rotation of the earth on its axis at 15^{O} per hour; morning negative, afternoon positive.

$$\omega = \frac{15^{O}}{hr}(t - 12) \qquad (4.10)$$

$$\omega = -56.25^{O}$$

The angle of incidence (θ): The angle between the beam radiation on a surface and the normal to that surface is given by;

$$Cos\,\theta = Sin\,\delta\,Sin\,\phi\,Cos\,\beta - Sin\,\delta\,Cos\,\phi\,Sin\,\beta\,Cos\,\Upsilon + Cos\,\delta\,Cos\,\phi\,Cos\,\beta\,Cos\,\omega + Cos\,\delta\,Sin\,\phi S\,\text{in}\,\beta\,Cos\,\Upsilon\,Cos\,\omega + Cos\,\delta\,Sin\,\beta\,Sin\,\Upsilon\,Sin\,\omega \quad (4.11)$$

$$Cos\,\theta = 0.0517621$$

$$\theta = 58.837^{O}$$

Zenith angle (θz): The angle between the vertical and the line to the sun, i.e., the angle of incidence of beam radiation on a horizontal surface.

$$Cos\,\theta z = Cos\,\phi\,Cos\,\delta\,Cos\,\omega + Sin\,\phi\,Sin\,\delta \quad (4.12)$$

$$Cos\,\theta z = 0.43965$$

$$\theta z = 63.92^{O}$$

Solar attitude angle (αS): The angle between the horizontal and the line to the sun, i.e., the complement of the zenith angle.

$$Cos\,\theta z = Sin(90 - \theta z) = Sin\,\alpha S$$

$$Sin\,\alpha S = Cos\,\phi\,Cos\,\delta\,Cos\,\omega + Sin\,\phi\,Sin\,\delta \quad (4.13)$$

$$Sin\,\alpha S = 0.43965$$

$$\alpha S = 26.08^{O}$$

4.3.1.3 Extraterrestrial Radiation on a Horizontal Surface

The extraterrestrial radiation measured on the plane is normal to the radiation on the nth day of the year Gon is (*John and William,1980*).

$$Gon = Gsc\left(1 + 0.033\,COS\frac{360n}{365}\right) \quad (4.14)$$

Here Gsc is the solar constant which is the energy from the sun per unit time received on a unit area of the outer surface. Gsc has a value of 1367W/m^2

$$Gon = 1406.6\frac{W}{m2}$$

At any point in time, the solar radiation incident on a horizontal plane outside of the atmosphere is the normal incident solar radiation as given by

$$Go = Gsc\left(1 + 0.033\ COS\frac{360n}{365}\right) Cos\ \theta z \qquad (4.15)$$

$$Go = Gon * Cos\ \theta z$$

$$Go = 618.42\frac{\mathrm{W}}{\mathrm{m2}}$$

Go = Solar extraterrestrial radiation incident on a horizontal plane

By integrating the above equation over the period from sunrise to sunset we obtain the daily extraterrestrial radiation on a horizontal surface, Ho.

$$Ho = \frac{24\times3600\ Gsc}{\pi}\left(1 + 0.033\ COS\frac{360n}{365}\right) \times \left(Cos\phi\ Cos\ \delta\ Sin\ \omega s + \frac{\pi\omega s}{180} Sin\phi\ Sin\ \delta\right) \qquad (4.16)$$

$$Ho = 31375334.83\frac{\mathrm{J}}{\mathrm{m2}}$$

Also, the extraterrestrial radiation on a horizontal surface for an hour (Io) is found by integrating equation for a period between hour angles $\omega 1$ and $\omega 2$

$$Io = \frac{12\times3600\ Gsc}{\pi}\left(1 + 0.033\ COS\frac{360n}{365}\right) \times \left[Cos\phi\ Cos\ \delta\ (Sin\ \omega 2 - Sin\ \omega 1) + \frac{\pi}{180}(\omega 2 - \omega 1)\ Sin\phi\ Sin\ \delta\right] \qquad (4.17)$$

For $\omega 1$ and $\omega 2$ 42.75 and 27.75 respectively

$$Io = 3791512\frac{J}{m^2}$$

4.3.1.4 Estimation of the Clear Sky Radiation

The atmospheric transmittance for beam radiation τ_b is given by

$$\tau_b = \alpha o + \alpha 1 \exp\left(\frac{-k}{Cos\theta z}\right) \qquad (4.18)$$

For tropical climates the constants αo ,$\alpha 1$, and k for standard atmosphere is given by

$$\alpha o = 0.95[0.4237 - 0.00821\,(6 - A)2] \quad (4.19)$$

$$\alpha 1 = 0.98[0.5055 + 0.00595\,(6.5 - A)2] \quad (4.20)$$

$$k = 1.02[0.2711 + 0.01858\,(2.5 - A)2] \quad (4.21)$$

Where, A = Altitude of the observer in kilometer

For $A = 2.254km$, $\alpha o = 0.293$, $\alpha 1 = 0.6005$, $k = 0.2776$ and $\tau_b = 0.612$

The empirical relationship between the transmission coefficient for beam and diffuse radiation for clear days be

$$\tau_d = \frac{G_d}{G_o} = 0.271 - 0.294\tau_b \quad (4.22)$$

$$\tau_d = 0.0909$$

$$I_b = \tau_b * I_o \quad (4.23)$$

$$I_b = 591.28\frac{W}{m^2}$$

$$I_d = \tau_d * I_o \quad (4.24)$$

$$I_d = 87\frac{W}{m^2}$$

$$I = I_b + I_d \quad (4.25)$$

$$I = 679.1\frac{W}{m^2}$$

The total solar radiation on the inclined surface for an hour as the sum of three terms

$$I_T = I_b R_b + I_d\left(\frac{1+cos\beta}{2}\right) + I\rho_g\left(\frac{1-cos\beta}{2}\right) \quad (4.26)$$

$$I_T = 784.45\frac{W}{m^2}$$

4.3.1.5 Basic Flat Plate Energy Balance

In a steady state, the useful energy output of a collector of area Ac is the difference between the absorbed solar radiation(S) and the thermal loss. From equation 2.1

$$Q_U = A_c[S - U_L(T_{pm} - T_a)]$$

The ambient temperature $Ta = 24\,°C$ and let's assume the mean absorber plate, $T_{pm} = 110\,°C$ and solar radiation in the area of study, $S = 784.5\frac{W}{m^2}$.

4.3.1.5.1 Collector Overall Heat Loss Coefficient

The overall heat loss coefficient in the collector is the sum of heat losses through the side, bottom, and top parts of the collector.

$$U_L = U_e + U_b + U_t \qquad (4.27)$$

$$U_b = \frac{k_i}{t_i} \qquad (4.28)$$

Where ki and ti are the thermal conductivity and thickness of the collector back insulation respectively.

$$U_b = 1$$

$$U_e = \frac{(UA)_{edge}}{A_c} \qquad (4.29)$$

$$U_e = 0.3$$

$$U_t = \left[\frac{N}{\frac{C}{T_{pm}}\left[\frac{T_{pm} - T_a}{N + f}\right]^e} + \frac{1}{h_w}\right]^{-1} + \frac{\sigma(T_{pm} + T_a)({T_{pm}}^2 + {T_a}^2)}{(\varepsilon_p + 0.00591Nh_w)^{-1} + \frac{2N + f - 1 + 0.133\varepsilon_P}{\varepsilon_g} - N}$$

.....(4.30)

Where:

$\mathcal{E}_g$ = Emittance of glass (0.88)

ε_p = Emittance of absorber plate (0.95)

h_w = Wind heat transfer coefficient $\left(14.82\frac{w}{m^{2\circ}\text{C}}\right)$=$5.7 + 3.8V$

σ = Stefan-Boltzmann constant $\left(5.67 \times 10^{-8}\frac{w}{m^2k^4}\right)$

V = Velocity of air $\left(2.4\frac{m}{s}\right)$

N = Number of glasses in collector (1)

T_{pm} = Mean plate temperature (assumed 110°C)

T_a = Ambient temperature(24°C)

C = $520(1 - 0.000051\beta^2)$, for 0° <β<70° = 516.3

e = $0.430(1 - \frac{100}{T_{pm}}$ = 0.3

f = $\left(1 + 0.089h_w - 0.1166h_w\varepsilon_p\right)(1 + 0.07866N)$ = 0.73

Then the overall heat loss coefficient be:

$$U_L = 5.5\ \frac{W}{m^2k}$$

The required amount of energy to raise the working fluid temperature is equal to the amount of energy that a solar collector could absorb. Then, heat gained in the generator is equal to the useful energy output of the collector ($Qg = Qu$) and taking values of $T_{pm} = 110°C$ and $T_a = 24°C$

$$Q_u = A_c\left[\text{S} - U_L\left(T_{pm} - T_a\right)\right]$$

$$A_c = 0.39\ m^2$$

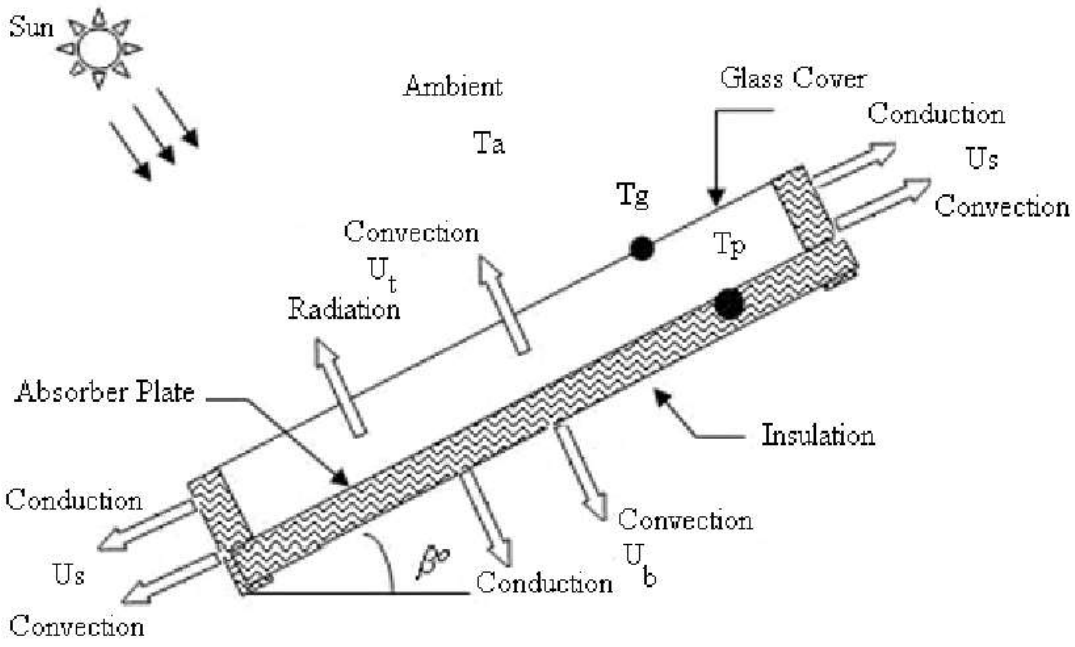

Figure 4. 1: Energy balance in flat plate collector(P. Vishwanath Kumar et all.2012n)

4.3.2 Design Analysis of Evaporator

The evaporator is the component of the system where the refrigeration effect takes place.

From cooling load analysis, we have Qe = 55 W

Now let's assume the following data

Condenser temperature, T_c = 40℃

Absorber temperature, T_a = 30℃

Generator temperature, T_g = 90℃

Evaporator temperature, T_e =-7℃

Generator or condenser pressure = 15.57 bar, from saturation table of ammonia corresponding to condenser temperature

Evaporator pressure = 3.28 bar, from ammonia saturation table of ammonia corresponding to evaporator temperature

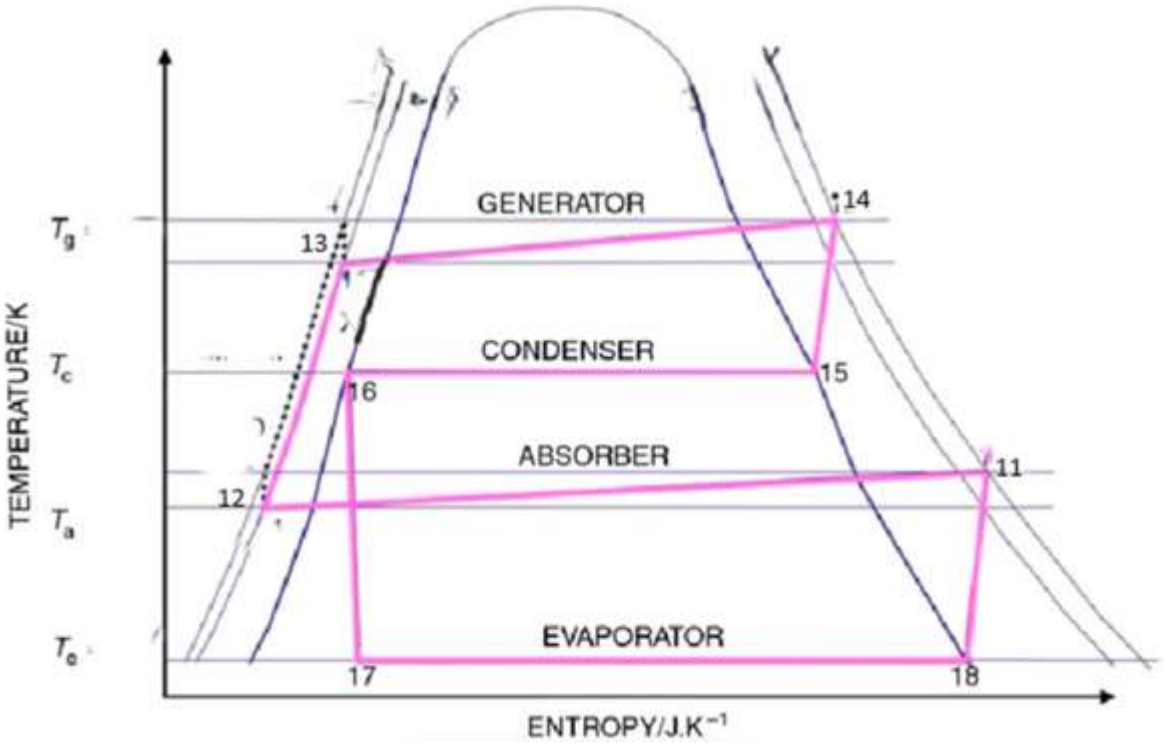

Figure 4. 2: T-S diagram of vapor absorption refrigeration system

Using enthalpy-concentration (see appendix) diagram of ammonia-water solution, we can find the concentration of weak NH_3 solution, $Xs = 0.36$ corresponding to Tg and Pc Using enthalpy-concentration diagram, we can also find the concentration of strong NH_3 solution, $Xs = 0.4$ corresponding to Ta and Pe

We have saturated vapor at the exit of the evaporator, so using the saturation table of ammonia at Pe and Te we have $h8 = 1453.8\frac{kJ}{kg}$.

Since we have isenthalpic expansion process $h6 = h7 = 390.6\frac{kJ}{kg}$, from the saturation table at Pc and Tc.

$$Qe = m_r(h_8 - h_7) \tag{4.31}$$

$$\dot{m}_r = \frac{0.0031kg}{min}$$

Mass Of solution (m_s) = Mass of refrigerant (m_r) + Mass of absorbent (m_w)

$$\dot{m}_s x_s = \dot{m}_r x_r + \dot{m}_w x_w \tag{4.32}$$

$$\dot{m}_w = 0.046 \frac{kg}{min}$$

$$\dot{m}_s = 0.049 \frac{kg}{s}$$

Estimate the area and length of the evaporator pipe using the LMTD method.

Let air inlet temperature to evaporator t_{h1} = 24℃

Air outlet temp, t_{h2} = 3℃

And evaporator temperature = -7℃

$$\theta 1 = t_{h1} - T_e = 31℃ \quad (4.33)$$

$$\theta 2 = t_{h2} - T_e = 10\,℃ \quad (4.34)$$

$$LMTD = \frac{\theta 1 - \theta 2}{\ln\left(\frac{\theta 1}{\theta 2}\right)} \quad (4.35)$$

$$LMTD = 18.56\,℃$$

Assuming, the convective heat transfer coefficient for the air side (natural convection), h_o = 25 W/m² and for ammonia inside the pipe, h_i = 100 W/m². The diameter of the pipe I get is, d = 0.017m therefore length of the pipe is:

$$U = \frac{1}{\frac{1}{h_i} + \frac{1}{h_o}} \quad (4.36)$$

$$Q_e = UA * LMTD \quad (4.37)$$

$$A = 0.148\,m^2$$

$$L = 2.7\,m$$

4.3.3 Design Analysis of Condenser

In the condenser, ammonia enters as saturated vapor and leaves as saturated liquid.

P_c = 15.57 bar

Tc = 40 °C

Using the saturated table for ammonia h_5 = 1490.4 KJ/kg and h_6 = 390.6 KJ/kg, then the heat rejected in the condenser will be:

$$Qc = mr * (h_5 - h_6) \quad (4.38)$$

$$Q_c = 56.89\, W$$

The condenser is air- cooled and to estimate the area and length of the condenser pipe, using the LMTD method.

Let air inlet temperature to condenser t_{a1} = 24℃

Air outlet temp, t_{a2} = 35℃

And condenser temperature = 40℃

$$\theta 1 = T_c - t_{a1} = 16℃$$

$$\theta 2 = T_c - t_{a2} = 5\,℃$$

$$LMTD = \frac{\theta 1 - \theta 2}{\ln\left(\frac{\theta 1}{\theta 2}\right)}$$

$$LMTD = 9.45\,℃$$

Assuming, the convective heat transfer coefficient for the air side (natural convection), h_o = 40 W/m² and for ammonia inside the pipe, h_i = 2500 W/m². The diameter of the pipe I get is, d = 0.017m therefore length of the pipe is:

$$U = \frac{1}{\frac{1}{h_i} + \frac{1}{h_o}}$$

$$Q_e = UA * LMTD$$

$$A = 0.152\, m^2$$

$$L = 2.8\, m$$

4.3.4 Design Analysis of Generator

Using enthalpy – concentration diagram for ammonia water solution

h_4 = hg at X=1 and Pc, h_4 = 1623.2 KJ/kg

h_3 =hf at X= 0.4 and Pe and temperature above Tc, h_3 = 270 KJ/kg

h_9 = hf at X=0.36 and Pc, h_9 = 355.69 KJ/kg

$$Q_g = m_r h_4 + m_w h_9 - m_s h_3 \quad (4.39)$$

$$Q_g = 120.97\ W$$

4.3.5 Design Analysis of Absorber

Using enthalpy – concentration diagram for ammonia water solution

h_1 = hg at X=1 and Pe, h_1 = 1595.59 KJ/kg

h_2 =hf at X= 0.4 and Pe, h_2 = 138.2 KJ/kg

h_{10} = hf at X=0.36 and P lower than Pc, h_{10} = 200 KJ/kg

$$Q_a = m_r h_1 + m_w h_9 - m_s h_2 \quad (4.40)$$

$$Q_a = 150.47\ W$$

4.3.6 Design Analysis of Capillary Tube

In the capillary tube, the pressure of the system needs to drop from condenser pressure to evaporator pressure, therefore the optimum capillary tube length can be calculated from the equation below (*White,1999*).

$$\Delta P = f \frac{L_p}{d} \frac{1}{2} \rho V^2 \quad (4.41)$$

Where the frictional factor *f* can be calculated using Renold's number

$$Re = \frac{4\dot{m}_r}{\pi \mu di} \quad (4.42)$$

With values of μ and di 1.5×10^{-4} and 3mm respectively the value of Re will be:

$$Re = 146$$

For laminar flow f can be calculated as follows:

$$f = \frac{64}{Re} \tag{4.43}$$

$$f = 0.43$$

Density of the liquid ammonia at mean temperature(16.5°C) = 808 kg/m³ and specific volume = ν = 0.0012m³/kg

$$L = 2.58\,m$$

4.3.7 COP of the System

The coefficient of performance of the system can be calculated as the ratio of refrigeration effect and energy input to the system as below:

$$COP = \frac{Q_e}{Q_g} \tag{4.44}$$

$$COP = 0.45$$

4.3.8 System Energy Efficiency

Energy efficiency is parameter for evaluating the success of the solar-powered vapor absorption refrigeration system. The overall energy efficiency of the system is determined by comparing the useful refrigeration output to the total energy input required to operate the system.

The solar energy input to the system for 6 hours radiation is calculated as:

$$E_{solar} = A_c \times I_t \times t \tag{4.45}$$

$$E_{solar} = 1834Wh$$

Where:

Ac = Collector area (m²)

It = Solar radiation incident on the collector (W/m²)

t = Time of collector exposure to radiation (hours)

E refrigeration = Q total

For a cooling load of 55 W over 6 hours, the energy consumed by the refrigeration system is: 330Wh

Finally, the energy efficiency ηenergy of the system is given by:

$$\eta_{energy} = \frac{E_{refrigeration}}{E_{solar}} \times 100\% \quad (4.46)$$

$$\eta_{energy} = 18\%$$

4.4 Refrigerant-absorbent preparation

The working fluid for the system is a 40% ammonia-water solution. Ammonia gas is carefully dissolved in water to create the solution. Different solution concentrations are prepared. A 34.7% solution is prepared by adding 2 liters of water and pouring ammonia gas into it until the volume reaches 3 liters. Subsequently, a 5-liter 40% solution is prepared.

During mixing, heat is released due to the exothermic reaction of ammonia absorption. To prevent ammonia loss, the solution is prepared in a cold-water bath, maintaining a low temperature. The 40% solution concentration is achieved by maintaining the correct ammonia-to-water ratio. The preparation takes place in the Moha factory.

Figure 4. 3: Preparation of ammonia solution

4.5 Manufacturing Prototype

The first step of the construction process involved sourcing and purchasing materials. This began by mapping out all design parameters and requirements. All selected materials had to meet or exceed every specification to ensure safety and proper system functionality.

4.5.1 Generator

In the system, the flat plate collector acts as a generator used to heat the strong aqua ammonia solution to the boiling temperature of the ammonia solution to produce ammonia vapor. The collector tilts 11° according to the latitude of Mekelle from the horizontal and it faces south to get a high amount of solar energy. The collector is 70x60 cm in size and has five rows of 20mm outer and 17mm inner diameter galvanized iron pipes connected using boring and welding to the 25mm outer diameter pipes in the upper and lower. In which the lower pipe acts as an inlet of the solution and the upper pipe acts as an outlet of the ammonia vapor. The pipes are attached to the black-painted aluminum absorber plate. At the back and sides of the collector, there is fiberglass insulation to reduce heat loss. The back and sides of the casing were combined using welding and the 6mm thick glass was attached to the casing by silicon sealant. Thermocouples and pressure gauges are installed at the outlet of the collector.

Figure 4. 4: Solar collector and generator

4.5.2 Condenser

The condenser is a heat exchanger in which the vapor from the generator changes to saturated liquid. In the condenser, heat is extracted from the refrigerant at constant pressure. The tube is 20mm outer and 17mm inner diameter and has 42 aluminum fines to facilitate heat transfer. The fins are 4x4mm and 1mm thick.

Figure 4. 5: Condenser with aluminum fin

4.5.3 Evaporator

The refrigerant at very low pressure and temperature from the capillary tube enters the evaporator and produces the cooling effect. The evaporator tube is the same as the tube of condenser in diameter. Heat transfer from the evaporator pipe to the products through the 1mm thick aluminum sheet. The pipe bends in some turns to fit in the compartment.

Figure 4. 6: Evaporator

4.5.4 Capillary Tube

The most commonly used refrigerant metering device is the capillary tube, a small hole tube connecting the outlet of the condenser to the inlet of the evaporator. A capillary tube has the advantage of extreme simplicity and no moving parts. The capillary tube is 3mm in diameter and 2.8m in length.

Figure 4. 7: Capillary tube

4.5.5 Separator

During regeneration not only ammonia vapor goes to the condenser some water vapor is carried with ammonia so to prevent water from entering the condenser this separator is important. It has an 88mm outer diameter and 4mm thickness.

Figure 4. 8: Separator

4.5.6 Absorber

The ammonia from the evaporator absorbs into the solution in the absorber. At the bottom of the absorber coil, there is an 88mm in diameter and 4mm thick absorber receiver. This receiver is also used in charging the solution to the system.

Figure 4. 9: Absorber

4.5.7 Compartment

The aluminum panel was cut into pieces to make the compartment 0.5x0.5x.04m. The pieces were combined using bolts. The compartment box is also put into a frame made of iron pipe to increase its height.

Figure 4. 10: Compartment

4.5.8 Valves and Connections

Different valves are used to restrict flow as well as inlet and outlet for the solution to the system and from the system respectively.

Figure 4. 11: Shutt off valves

4.5.9 Measuring Devices

To measure the input and output values of temperature thermocouples were installed at the inlet and outlet part of the components and two pressure gauges were installed at the exit of the generator and the exit of the evaporator. A data logger was used to read the temperature outputs from thermocouples.

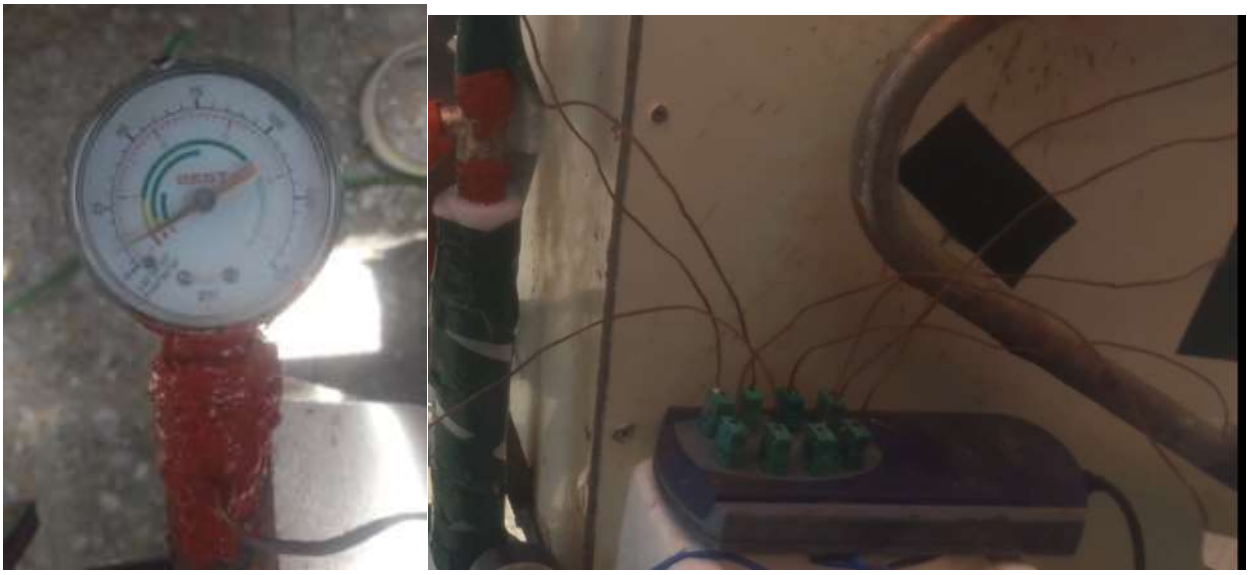

a. Pressure gauge *b. Thermocouple*

Figure 4. 12: Measuring devices

4.5.10 Insulation and Sealants

To prevent heat loss insulation materials like thermos-cool and fiberglass were used. In addition, epoxy, silicon sealant, and gasket maker were used to prevent leakage of refrigerant through thermocouples.

a. Epoxy *b. Gasket maker* *c. Silicon sealant*

Figure 4. 13: Sealing materials

a. Fiberglass *b. Thermocol*

Figure 4. 14: Insulation

4.5.11 Vapor Absorption Refrigeration System

Figure 4.15 shows the overall model of the system. In this system, different components of the system are combined by welding as well as using epoxy and a gasket maker at the connections of the thermocouple and pressure gauge.

Figure 4. 15: The vapor absorption refrigeration system

4.6 Solution Filling Procedure

The solution was added to the system through the valve in the absorber tank.

Figure 4. 16: Solution-filling procedure

4.7 Experimental Setup

The experimental setup consisted of the following components:

Flat Plate Solar Collector: Used to provide heat to the generator for the ammonia-water solution.

Absorption Refrigeration System: Including the generator, absorber, condenser, evaporator, and capillary tube.

Measurement Instruments: Thermocouples and pressure gauges were used to measure temperatures and pressures at various points in the system.

Pressure gauges and thermocouples were installed at various locations within the system to monitor operational parameters. The first pressure gauge was positioned between the generator outlet and condenser inlet to measure generator and condenser pressures, while the second pressure gauge was placed between the evaporator outlet and absorber inlet to monitor evaporator and absorber pressures.

Thermocouples were mounted at key locations, including the absorber plate, as well as at the inlet and outlet positions of the generator, condenser, capillary tube, evaporator, and absorber pipes to record temperature variations across system components. An additional thermocouple was installed inside the compartment to measure internal compartment temperature.

4.8 Cost Estimation

Table 4.2: Cost estimation of components

NO	Part	Quantity	Estimated Price (Birr)
1	Galvanized iron pipe	18m	3000
2	Aluminum sheet	1x 2 m	700
3	Aluminum panel	2.4x1.2 m	2500
4	Iron sheet	1x 2 m	1500
5	Absorber tank	1m	850
6	Capillary tube	3m	300
7	Fiberglass	3Kg	750
8	Glass	0.4m²	300

9	Epoxy	2	800
10	Gasket maker	2	400
11	Valves	4	600
12	Pressure gauge	2	3000
13	Plaster	1	70
14	Silicon sealant	1	250
15	Bolts	30	30
16	Aluminum foil	1	70
17	Total		15050

Other than the costs listed in Table 4.1 there were also labor costs to build the system and transport costs.

5. RESULT AND DISCUSSION

5.1 Introduction

The experimental investigation of the ammonia-water absorption refrigeration system encountered operational challenges due to ammonia leakage, which affected pressure and temperature measurements across system components. Despite these limitations, the obtained data provides valuable insights into the system's performance characteristics under partial operating conditions. This section presents the key observations from the experimental trials and discusses their implications relative to theoretical expectations and findings from comparable studies.

5.2 Design Results

In the design analysis part, different parameters to achieve the construction of the system were obtained. Table 5.1 shows some of these parameters.

Table 5. 1: The absorption refrigeration system design parameter values

Parameter	Value	Unit
Solar radiation	784.5	W/m²
Collector area	0.39	m²
Cooling capacity	55	W
Heat added to the generator	120.97	W
Heat rejected in condenser	56.89	W
Heat rejected in the absorber	150.47	W
Refrigerant mass flow rate	0.186	Kg/hr.
Solution flow rate	2.97	Kg/hr.
Solution concentration	40	%
Length of condenser	2.8	M
Length of evaporator	2.7	M
Length of capillary tube	2.8	M
COP	0.45	-

Table 5.1 provides various parameters and their corresponding values for a solar-powered cooling system. The system utilizes solar radiation with an intensity of 784.5 W/m² and a collector area of 0.39 m² to achieve a cooling capacity of 55 W.

The system's energy balance is as follows: 120.97 W of heat is added to the generator, 56.89 W is rejected in the condenser, and 150.47 W is rejected in the absorber. The system operates with a

refrigerant mass flow rate of 0.186 kg/hr. and a solution flow rate of 2.97 kg/hr. The solution concentration is 40%. In addition, the total volume of the compartment was 48 liters, and 30 liters of the total volume occupied by the product.

The dimensions of the system's components are: condenser length of 2.8 m, evaporator length of 2.7 m, and capillary tube length of 2.8 m. The system's coefficient of performance (COP) is 0.45.

5.3 Experimental Results

The system was initially tested for leaks using water, and some leaks were found in welded joints. To address this, the welding system was revised, and epoxy and gasket maker were added to the connections. The first 8 tests used a 25% ammonia solution from Mekelle University and were conducted from September 21-24, 2020. These initial tests were hindered by several factors, including a faulty pressure gauge, inaccurate thermocouple placement, and inconsistent data logger usage.

Test 9, which began on September 25, 2020, incorporated improvements based on the lessons from the initial tests. Temperature variations were observed in the components, as shown in Figure 5.1. The data logger failed after an hour, but the generator and absorber plate temperatures were recorded above 60°C and 80°C, respectively.

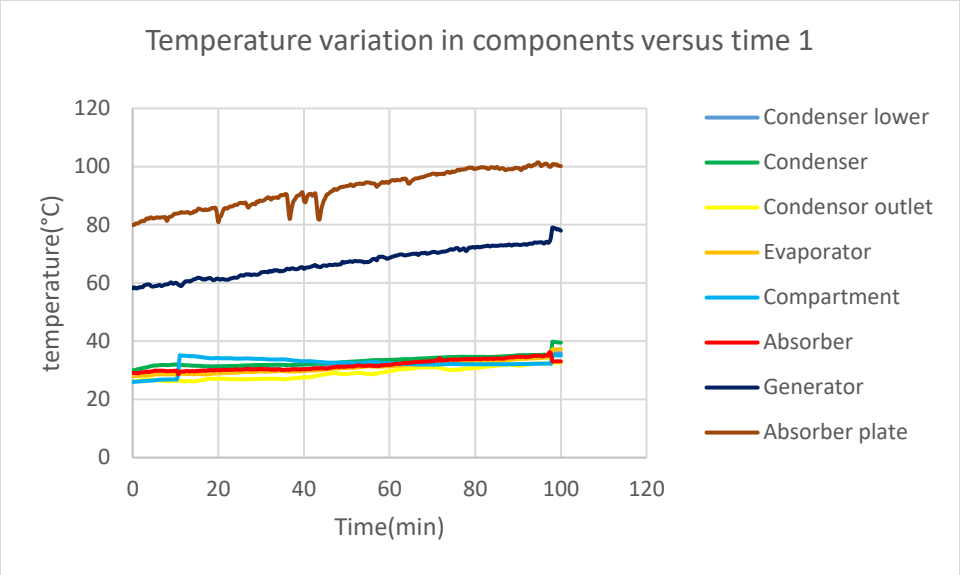

Figure 5. 1: Temperature variation in components try 1

The graph in Fig 5.1 shows how the temperatures of different components in a refrigeration system change over time. The x-axis represents time in minutes, while the y-axis indicates temperature in degrees Celsius.

The graph displays the temperature variations of the condenser lower, condenser, condenser outlet, evaporator, compartment, absorber, generator, and absorber plate. Initially, all components start at relatively low temperatures. As time progresses, the temperatures of most components increase, with the absorber plate and generator reaching the highest temperatures around 100 minutes which is 100°C and 80°C respectively.

The temperatures of the evaporator, compartment, absorber and condenser also rise over time. The temperature of condenser reaches 40°C but the evaporator temperature was not achieved. The analysis of the results suggests that the concentration and quantity of the ammonia solution may be critical factors affecting the system's performance.

Tests 10 and 11 followed the same procedure as Test 9. Test 12 Conducted on September 29, 2020, at 11:10 AM. Used a 40% ammonia solution. Temperature variations were recorded as shown in Figure 5.2.

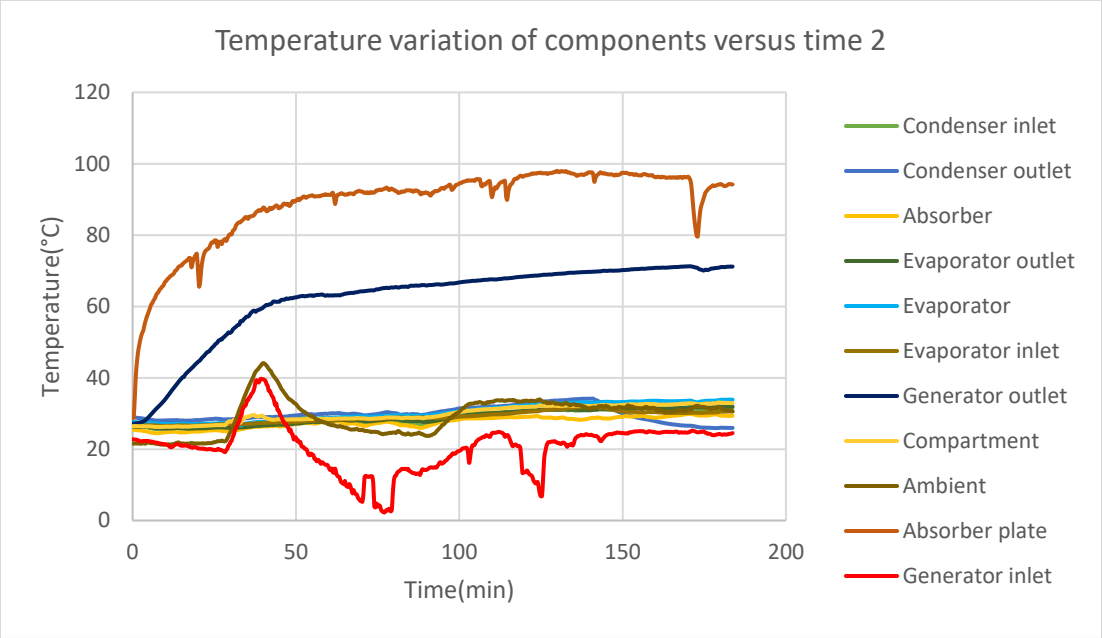

Figure 5. 2: Temperature variation in components for try 2

Fig 5.2 shows how the temperatures of various components in a refrigeration system change over time. The x-axis represents time in minutes, while the y-axis indicates temperature in degrees Celsius.

The graph shows the temperature variations of the condenser inlet, condenser outlet, absorber, evaporator outlet, evaporator, evaporator inlet, generator outlet, compartment, ambient temperature, absorber plate, and generator inlet. Initially, all components start at relatively low temperatures. As time progresses, the temperatures of most components increase. The absorber plate reaches the highest temperatures, followed by the generator.

The generator temperature increased from 27°C to 72°C, and the absorber plate temperature increased from 28°C to 97°C. A temperature drop in the absorber plate was observed due to cloud cover. The test was hindered by ammonia gas leakage through a tiny hole drilled from thermocouple installation and around the pressure gauge connections, despite sealing efforts with epoxy sealant.

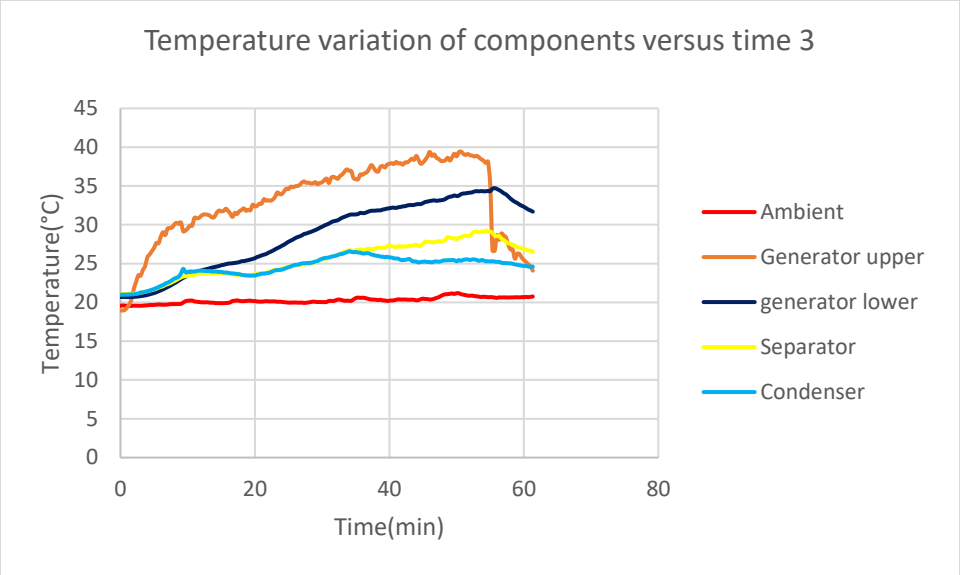

Figure 5. 3: Temperature variation in components for try 3

Fig 5.3 shows how the temperatures of various components in a refrigeration system change over time. The x-axis represents time in minutes, while the y-axis indicates temperature in degrees Celsius.

The graph shows the temperature variations of the ambient temperature, generator upper, generator lower, separator, and condenser. Initially, all components start at relatively low temperatures. As time progresses, the temperatures of most components increase. The generator reaches the highest temperatures. The condenser and ambient temperature show a gradual increase but remain at lower levels compared to the generator components and the separator.

Fig 5.4 shows the relationship between the pressure and temperature within a generator. The x-axis represents pressure in kilopascals (kPa), while the y-axis indicates temperature in degrees Celsius (°C).

The graph shows that as the pressure inside the generator increases, the temperature also increases. Initially, there is a sharp increase in temperature with a small increase in pressure. However, as the pressure continues to rise, the rate of temperature increase slows down. This trend suggests that the generator's temperature is more sensitive to pressure changes at lower pressures compared to higher pressures.

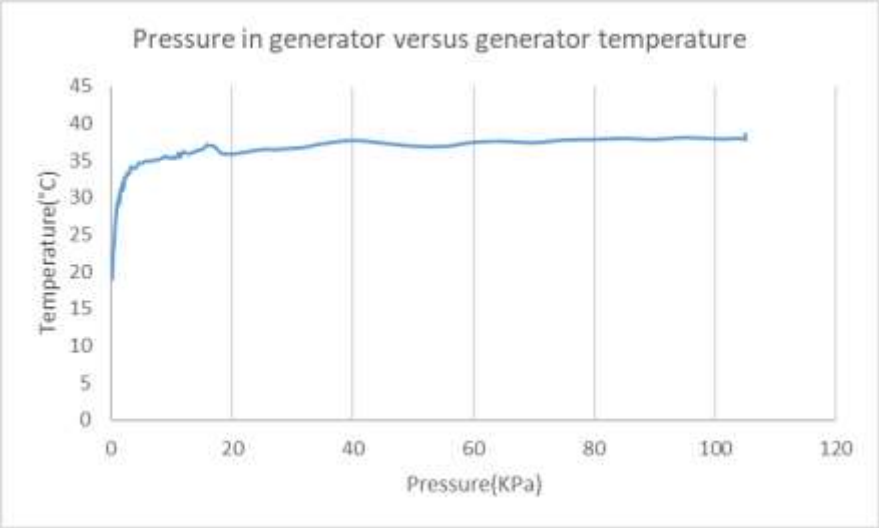

Figure 5. 4: Pressure variation in generator with an increase in generator temperature

The comparison between the predicted and experimental results for the generator and absorber plate temperatures reveals a discrepancy. While the design analysis predicted temperatures of 90°C and 110°C, respectively, the experimental tests yielded 80°C and 100°C. The factors contributing to this discrepancy are identified as cloud cover and ammonia gas leakage. These factors negatively impacted the system's performance, preventing it from reaching the expected temperatures.

Despite these challenges, the obtained temperatures were sufficient to achieve the desired condenser pressure. This suggests that while the system's overall performance was affected, it was still able to maintain essential operational parameters.

While the condenser temperature reached the expected 40°C, the anticipated condenser pressure was not attained. The primary reason for this discrepancy is attributed to excessive ammonia leakage and potential issues with the pressure gauge's proper functioning. These factors hindered the system's ability to condense sufficient refrigerant in the condenser, leading to insufficient pressure drop in the capillary tube and preventing the attainment of the target 3°C compartment temperature.

5.3.1 Predicted Results Based on Previous Studies

The inability to obtain all expected test data due to ammonia leakage necessitates the prediction of condenser pressure and evaporator temperatures for the system. This prediction is based on the

measured generator temperature of 80°C and condenser temperature of 40°C. Reference to similar studies on ammonia-based vapor absorption refrigeration systems provides guidance for this estimation. Numerous investigations of solar-powered absorption refrigeration systems utilizing ammonia as the refrigerant indicate characteristic operating ranges for condenser and evaporator temperatures relative to the generator temperature.

According *(Mondal et al., 2015)*, the generator temperature was typically between 95°C and 102°C with generator temperature 4.5-12bar. In this range the condenser temperature was found to be around 25°C to 34°C. The evaporator temperature was found to be around 4°C to 8.5°C, depending on the system's cooling capacity and operational parameters.

According to *(Tangka & Kamnang, 2006)*, with a generator temperature of 100°C, the evaporator temperature was set to 11°C.

According to *(Sarbu & Sebarchievici, 2013)*, review of solar cooling methods at a generator temperature of 65-70°C, the evaporator temperature be -7°C.

According to *(Siddiqui & Said, 2015)*, also referring table in appendix, it is feasible to achieve an evaporator temperature of up to -70°C for a cooling load between 300-1100 KJ/kg. This can be accomplished with a generator temperature range of 130-180°C, an absorber temperature range of 15-35°C, a condenser temperature range of 10-30°C, a COP of 0.2-0.65, and an operating pressure of 15 bar.

According to *(A. Al-Hemiri & Deaa Nasiaf, 2010),* in which describes the use of direct solar energy in absorption refrigeration employing NH3 – H2O system, typical ammonia-water absorption systems at a generator temperature of 92-97°C, the condenser temperature typically ranged between 30°C and 35°C with pressure 10bar. The evaporator temperature ranges from 5°C to 10°C.

Considering the previous similar studies, the predicted evaporator temperatures for a solar-powered ammonia absorption refrigeration system with a generator temperature of 80°C would be 5°C and up to 15bar condenser pressure could be achieved in the absence of ammonia leakage.

6. CONCLUSION AND RECOMMENDATION

6.1 Conclusion

In this study, a vapor absorption refrigeration system using solar energy was developed manufactured, and experimentally tested. From the solar radiation calculation, 784.5 W/m² solar radiation was obtained and used in calculating the area of the flat plate collector which is 0.39 m². The capacity of the system was 55 W from the cooling load analysis and the heat added in the generator was computed as 120.9 W in which turns COP of the system was 0.45. Comparing to the COP computed from previous studies which varies 0.1-0.4 the computed COP was good. From the experimental results, the generator and absorber plate temperature reached 80°C and 100°C respectively which was enough for generation. The pressure exhibits a slight initial increase, but subsequent ammonia gas leakage causes it to decrease, preventing the achievement of expected pressure and temperature levels in the system components. Insufficient ammonia solution prevents obtaining precise experimental results. However, the trial suggests that with proper welding and effective system sealing, the desired performance could be achieved, making the system viable for off-grid applications.

6.2 Recommendation

This study demonstrates the potential for preserving medicine and agricultural products in off-grid areas using solar-operated refrigeration systems. To enhance the system's performance and reliability, the following recommendations are proposed:

- To prevent leakage, employ precise welding techniques to ensure a high-quality seal during the manufacturing and prototype construction process. Conduct leakage tests using appropriate gases to minimize refrigerant loss and improve system efficiency.
- To optimize the system for continuous operation by adding energy storage materials. This enhancement would enable the system to function effectively during nighttime or periods of low solar radiation.

REFERENCE

1. Beyene G. 2018. *The Challenges and Prospects of Electricity Access in Ethiopia*.
2. IEA.2020*, Ethiopia—Access to electricity (% of population)*. https://www.indexmundi.com/facts/ethiopia/indicator/EG.ELC.ACCS.ZS
3. Tangka, J. K., & Kamnang, N. E. (2006). *Development of a simple intermittent absorption solar refrigeration system*. International Journal of Low-Carbon Technologies, 1(2), 127–138. https://doi.org/10.1093/ijlct/1.2.127
4. Ethiopian Federal Ministry of Health.2015. "*Ethiopian National Expanded Program on Immunization Comprehensive* Multi-Year Plan 2016 - 2020," pp. 1–104.
5. The Beam Magazine.2019. *The cold truth about Ethiopia's nutrition gap.* https://medium.com/thebeammagazine/the-cold-truth-about-ethiopias-nutrition-gap-8401b6260f70
6. R. S. Khurmi, J. Gupta.2009. *A Textbook of Refrigeration and Air Conditioning.*
7. Dincer, I., & Ratlamwala, T. A. H. (2016). *Integrated Absorption Refrigeration Systems*. Springer International Publishing. https://doi.org/10.1007/978-3-319-33658-9
8. Wilsdon, C. (2009). *Science in the Real World: How Do Refrigerators Work?* (1st ed). Chelsea House.
9. World Health Organization & United Nations Children's Fund (UNICEF). (2015). *Introducing solar-powered vaccine refrigerator and freezer systems: A guide for managers in national immunization programs*. World Health Organization. https://iris.who.int/handle/10665/195778
10. John A. Duffie, William A. Beckman. 1980.Solar Engineering of Thermal Processes
11. Laveyne, J. I., Bozalakov, D., Van Eetvelde, G., & Vandevelde, L. (2020). *Impact of Solar Panel Orientation on the Integration of Solar Energy in Low-Voltage Distribution Grids.* International Journal of Photoenergy, 2020, 1–13. https://doi.org/10.1155/2020/2412780
12. D. Yogi Goswami, F. Kreith,Jan F. Kreider. 2000. *Principles of solar engineering*.

13. Shirazi, A., Taylor, R. A., Morrison, G. L., & White, S. D. (2018). *Solar-powered absorption chillers: A comprehensive and critical review.* Energy Conversion and Management, 171, 59–81. https://doi.org/10.1016/j.enconman.2018.05.091
14. Wang, S. K. (2000). *Handbook of air conditioning and refrigeration* (2nd ed). McGraw-Hill.
15. *CIBSE Journal.2009. Module 10: Absorption refrigeration*. https://www.cibsejournal.com/cpd/modules/2009-11/
16. EnggCyclopedia.2012. *Vapor Compression Refrigeration (VCR)*. https://enggcyclopedia.com/2012/01/typical-vapor-compression-refrigeration-cycle-vcr/#google_vignette
17. Dinçer, İ. (2003). *Refrigeration systems and applications*. Wiley.
18. Sachin T.2020.*Types of Refrigeration System—Classification of Refrigeration*. https://learnmech.com/types-of-refrigeration-system-classification-of-refrigeration/
19. EE IIT, Kharagpur, India.2008. *Refrigeration and Air Conditioning-IIT Kharagpur Notes | PDF | Refrigeration | Heat Pump*. https://www.scribd.com/doc/25369918/Refrigeration-and-Air-Conditioning-IIT-Kharagpur-Notes
20. Mondal, A., Alam, D., & Islam, M. A. 2015. *Design & Construction of a Solar Driven Ammonia Absorption Refrigeration System*.
21. Kim D. S. & Infante Ferreira C. A. (2008). *Solar refrigeration options – a state-of-the-art review.* International Journal of Refrigeration, 31(1), 3–15. https://doi.org/10.1016/j.ijrefrig.2007.07.011
22. Sarbu I., & Sebarchievici C. (2013). *Review of solar refrigeration and cooling systems.* Energy and Buildings, 67, 286–297. https://doi.org/10.1016/j.enbuild.2013.08.022
23. Wageiallah Mohammed, O., & Yanling, G. (2017). *Comprehensive Parametric Study of a Solar Absorption Refrigeration System to Lower Its Cut In/Off Temperature*. Energies, 10(11), 1746. https://doi.org/10.3390/en10111746
24. Siddiqui, M. U., & Said, S. A. M. (2015). *A review of solar powered absorption systems.* Renewable and Sustainable Energy Reviews, 42, 93–115. https://doi.org/10.1016/j.rser.2014.10.014

25. A. Al-Hemiri, A., & Deaa Nasiaf, A. (2010). T*he use of direct solar energy in absorption refrigeration employing NH3 – H2O system*. Iraqi Journal of Chemical and Petroleum Engineering, 11(4), 13–21. https://doi.org/10.31699/IJCPE.2010.4.2
26. Shahad, H. A. K., & Hamzah, D. A. 2015. *Investigation on an Intermittent Absorption Refrigeration prototype powered by Solar Irradiation*. *8*(4).
27. Dara, J. E., Okechukwu, K., Obinna, U. N., Chinwuko, C. E., & Ubachukwu, O. A. (2013). *Evaluation of a Passive Flat-Plate Solar Collector*.
28. American Society of Heating, Refrigerating and Air-Conditioning Engineers (Ed.). (2010). *2010 ASHRAE handbook: Refrigeration* (Inch-pound ed). American Society of Heating, Refrigerating and Air Conditioning Engineers.
29. Greentech Renewables. (2010, November 24). *Calculating Your Optimal Azimuth Angle* https://www.greentechrenewables.com/article/calculating-your-optimal-azimuth-angle
30. P. Vishwanath Kumar et all.2012. *Optimization of design and operating parameters on the year-round performance of a multi-stage evacuated solar desalination system using transient mathematical analysis.* International Journal of Energy and Environment Volume 3, Issue 3, 2012 pp.409-434 https://www.researchgate.net/publication/ 277892685
31. White F.*1999. Fluid mechanics, 4th edition*.

APPENDIX

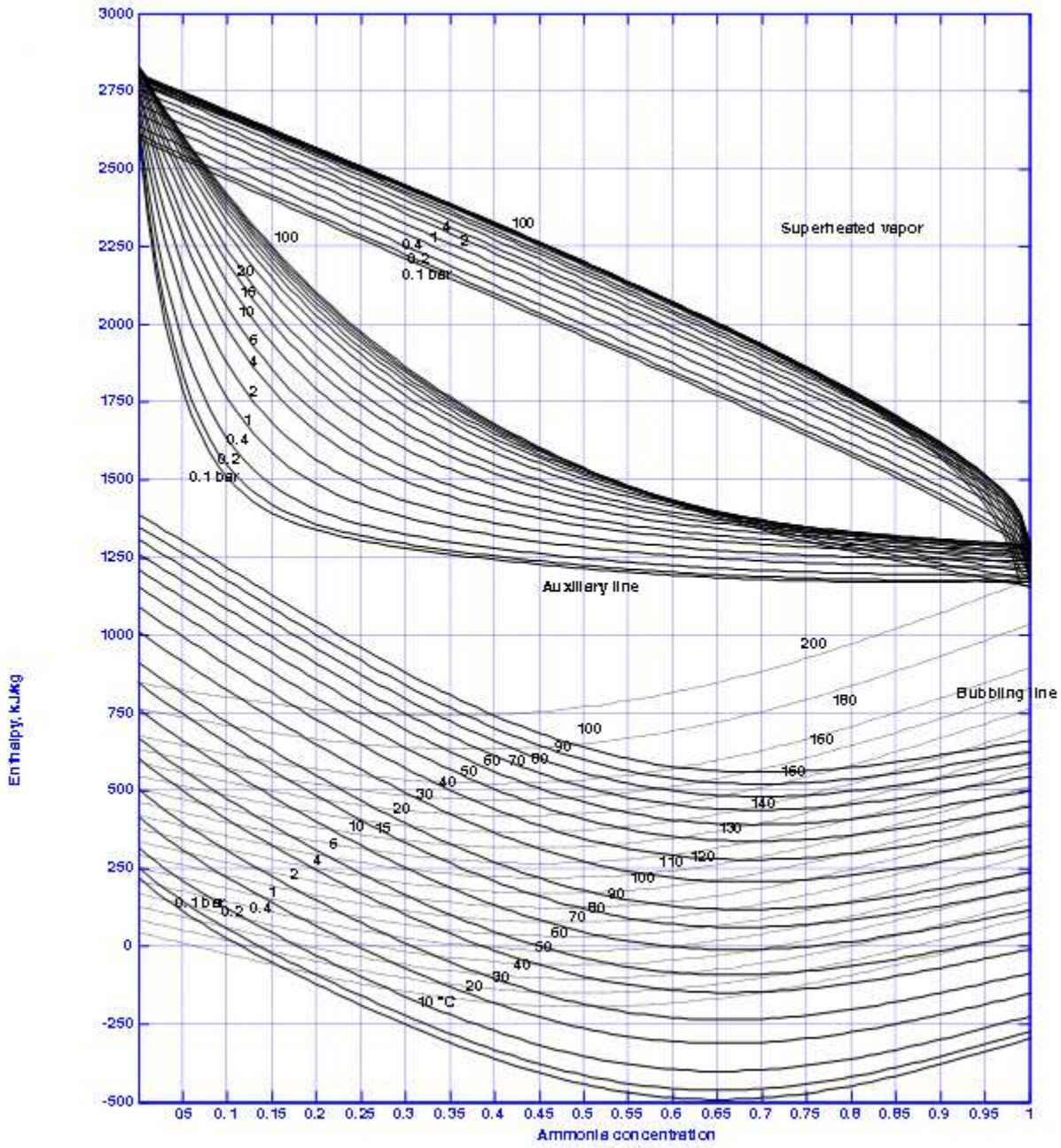
Enthalpy, kJ/kg
Ammonia concentration
Superheated vapor
Auxiliary line
Bubbling line
0.1 bar
-10 °C

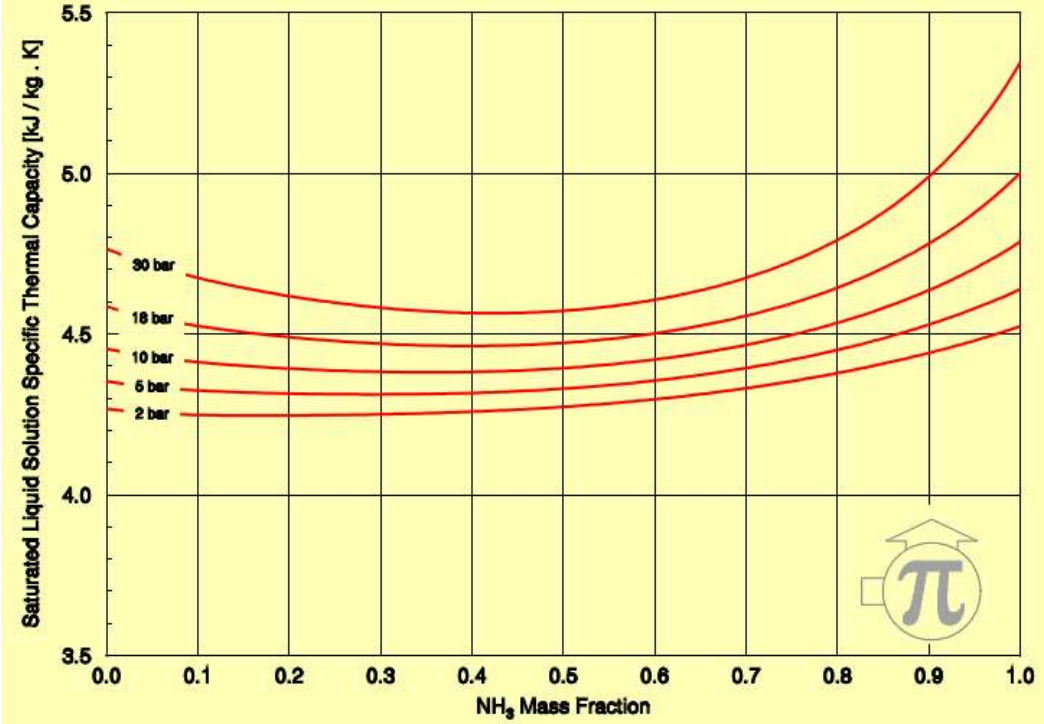
Saturated Liquid Solution Specific Thermal Capacity [kJ / kg . K]
5.5
5.0
4.5
4.0
3.5
30 bar
18 bar
10 bar
5 bar
2 bar
0.0
0.1
0.2
0.3
0.4
0.5
0.6
0.7
0.8
0.9
1.0
NH3 Mass Fraction

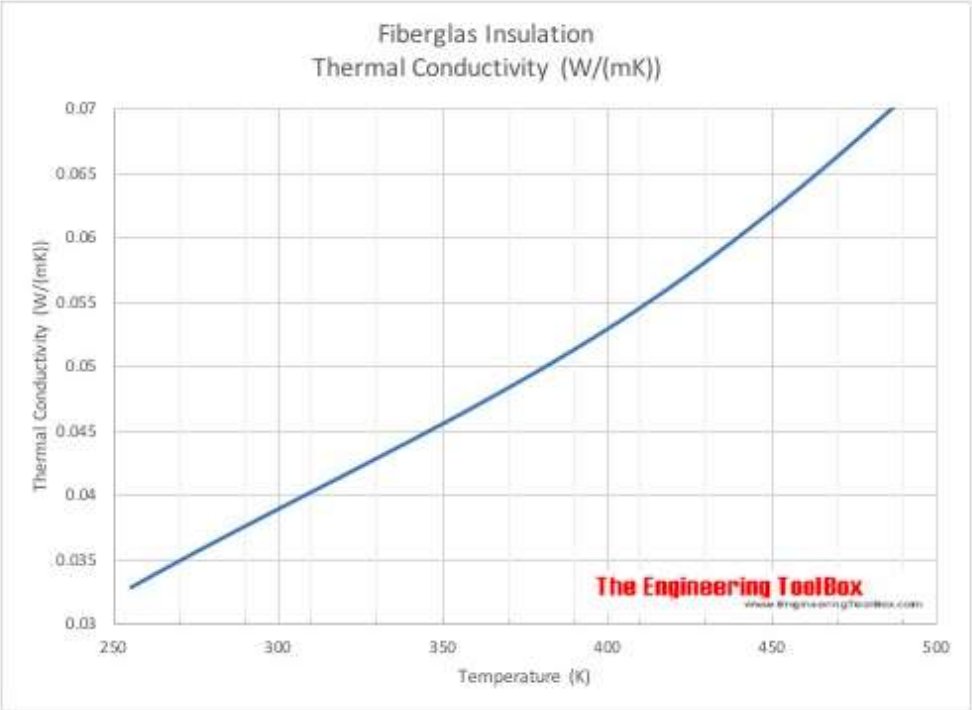
Fiberglas Insulation
Thermal Conductivity (W/(mK))
Thermal Conductivity (W/(mK))
0.07
0.065
0.06
0.055
0.05
0.045
0.04
0.035
0.03
250
300
350
400
450
500
Temperature (K)
The Engineering ToolBox

Iron - Density, Specific Heats and Thermal Conductivities vs. Temperatures

T (K)	ρ (kg/m³)	c (kJ/kg K)	k (W/m K)
100	7900	0.216	134
150	7890	0.324	104
200	7880	0.384	94
250	7870	0.422	87
300	7860	0.450	80
400	7830	0.491	70
600	7760	0.555	55
800	7690	0.692	43
1000	7650	1.034	32
1200	7620		28
1400	7520		31
1600	7420		
1800	7420		

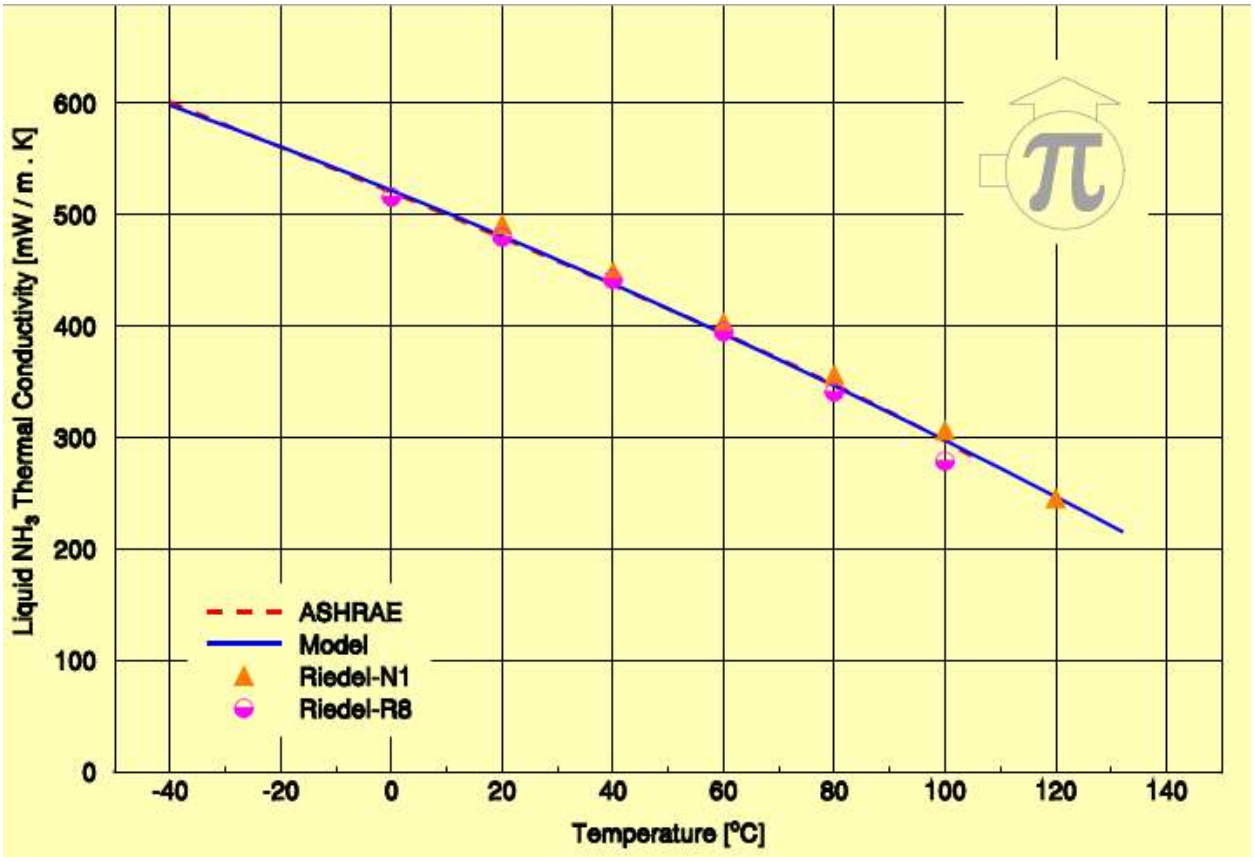

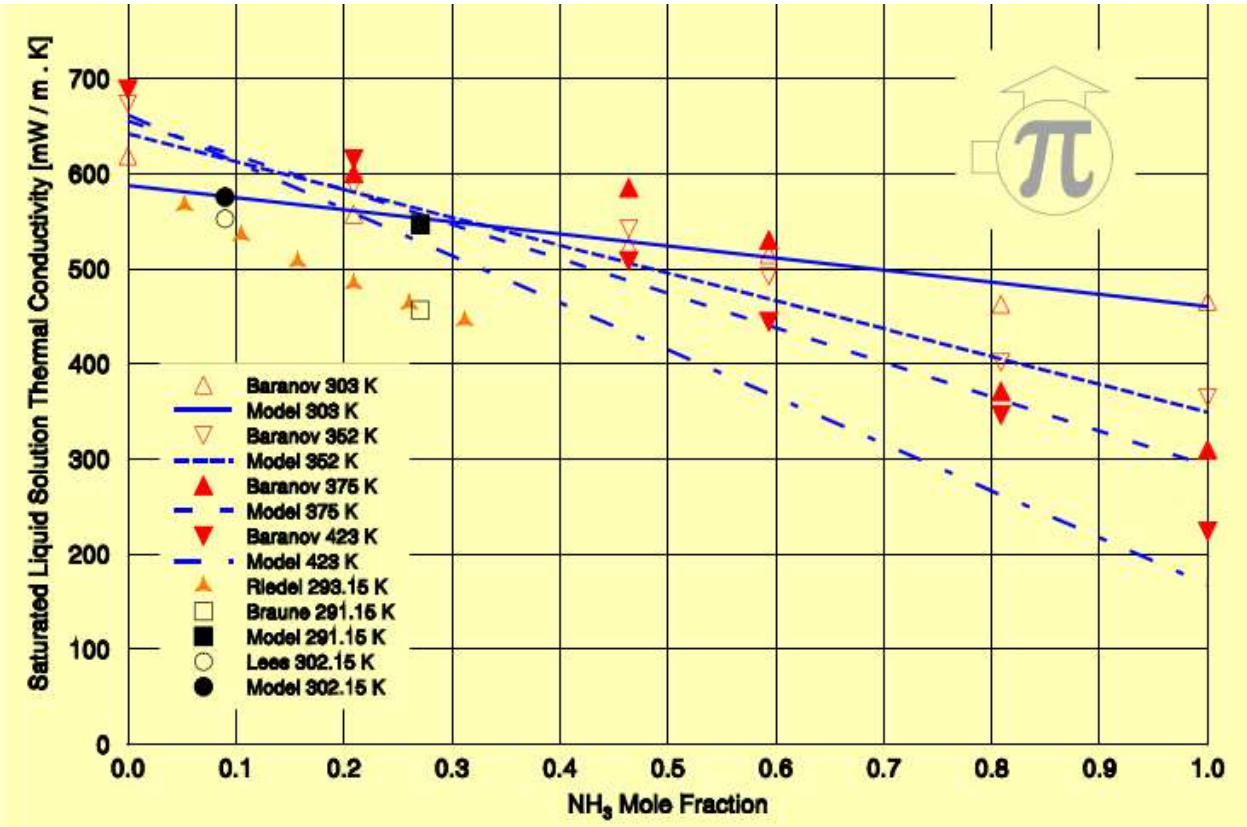
Saturated Liquid Solution Thermal Conductivity [mW / m . K]
NH3 Mole Fraction
Baranov 303 K
Model 303 K
Baranov 352 K
Model 352 K
Baranov 375 K
Model 375 K
Baranov 423 K
Model 423 K
Riedel 293.15 K
Braune 291.15 K
Model 291.15 K
Lees 302.15 K
Model 302.15 K

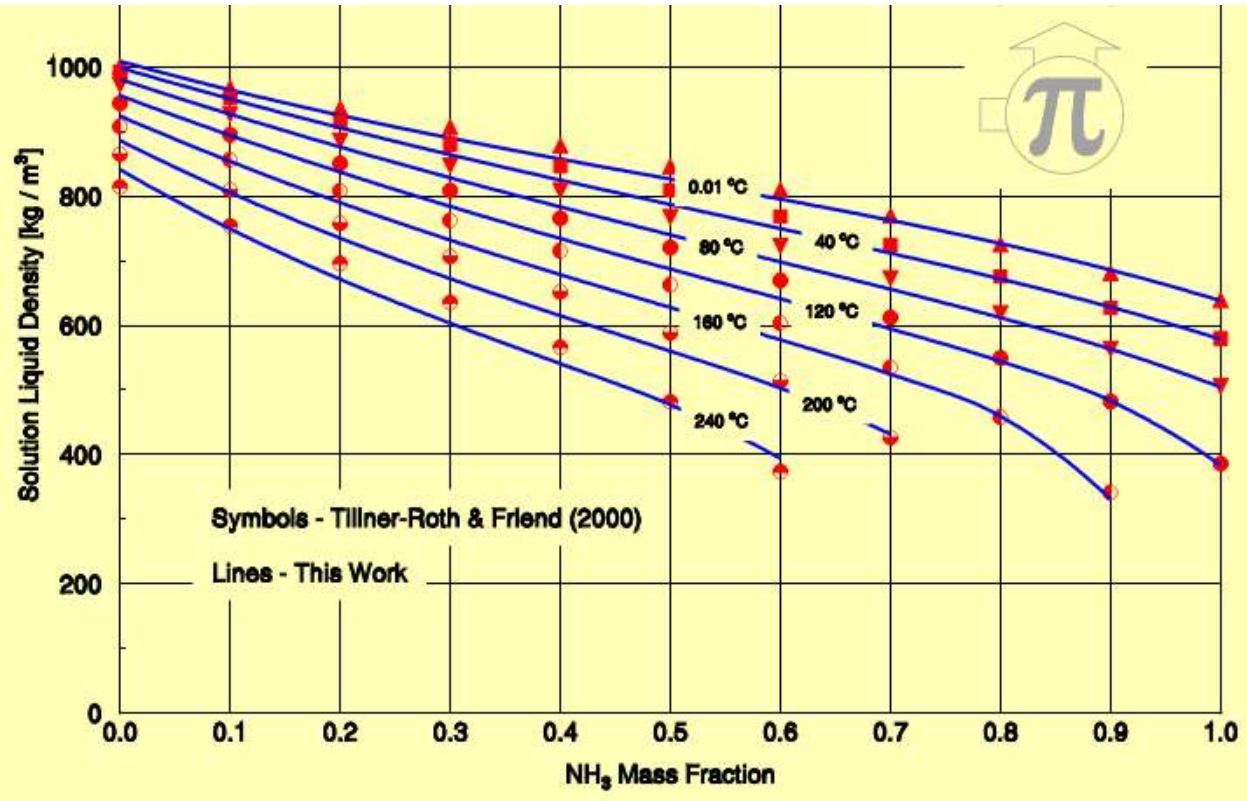
Solution Liquid Density [kg / m3]
NH3 Mass Fraction
0.01 °C
40 °C
80 °C
120 °C
160 °C
200 °C
240 °C
Symbols - Tillner-Roth & Friend (2000)
Lines - This Work

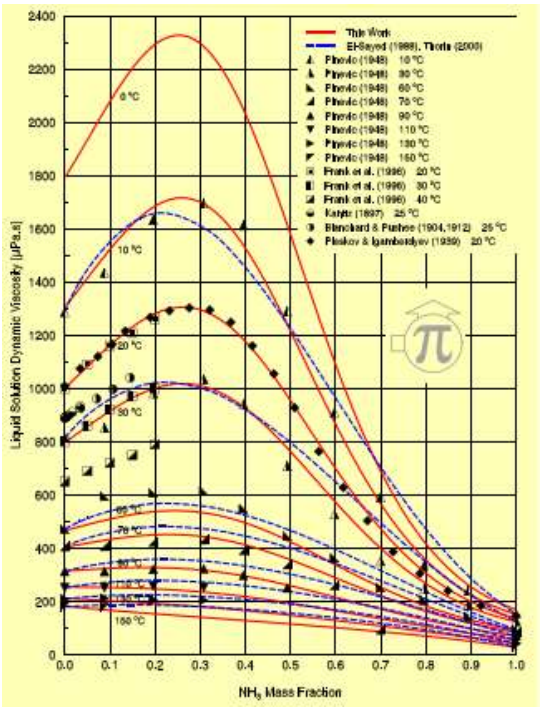

Refs.	Research type	Working pair	Type of operation	Cooling load	Temperatures (°C)				Operating pressure	COP
					Generator	Absorber	Condenser	Evaporator		
Raghuvanshi and Maheshwari [27]	Simulation (MATLAB)	Aqua-ammonia	Continuous operation	62.7 kW	50	20	50	2.5	20.33 bar	0.227
Said et al. [28]	Simulation (EES)	Aqua-ammonia	Continuous operation and intermittent operation	5 kW for 24 h i.e. 120 kW-h	120	45	45	−9	Not reported	0.427 (continuous operation) 0.23 (Intermitten operation)
Darwish et al. [29]	Simulation (ASPEN)	Aqua-ammonia	Continuous operation	10 kW	166	40	40	−7	15.55 bar	0.45
Sencan [32,33]	Simulation (artificial neural networks)	Aqua-ammonia	Continuous operation	Not reported	60–90	20–40	20–40	2.5–7.5	Not reported	0.67–0.81
Bangotra and Mahajan [35]	Simulation	Aqua-ammonia	Continuous operation	10.548 kW	120	52	54	2	10.7 bar	0.2079
Lavanya and Murthy [36]	Simulation	Aqua-ammonia	Continuous operation	116.9 W	90	28	34	−18	14 bar	0.6
Chua et al. [38]	Simulation	Aqua-ammonia	Continuous operation	6.17 kW	145	45	51	3.5	20.7 bar	0.519
Lostec et al. [39]	Simulation	Aqua-ammonia	Continuous operation	3 kW	72	17	17	−11	8 bar	0.69
Caciula et al. [40]	Simulation	Aqua-ammonia	Continuous operation	100 kW	70–150	30	30	−3 to 6	Not reported	0.6–0.73

Table 1 (continued)

Refs.	Research type	Working pair	Type of operation	Cooling load	Temperatures (°C)				Operating pressure	COP
					Generator	Absorber	Condenser	Evaporator		
Cai et al. [41]	Simulation (dynamic)	Aqua-ammonia	Continuous operation	1109 kW	100	30	40	10	15.6 bar	0.642
Kim and Park [42]	Simulation (dynamic)	Aqua-ammonia	Continuous operation	10.5 kW	165	58.6	54.5	4.8	21.68 bar	0.557
Kim et al. [43]	Simulation (dynamic)	Aqua-ammonia	Continuous operation	10 kW	120	30	30	12.5	17.5 bar	Not reported
Ozgoren et al. [44]	Simulation (dynamic)	Aqua-ammonia	Continuous operation	3.5 kW	110	36–52	36–52	10	Not reported	0.243–0.454 (for cooling) 1.243–1.454 (for heating)
Lin et al. [45]	Simulation	Aqua-ammonia	Continuous operation	5 kW	80	46 (Low pressure) 50 (Medium pressure)	42	10	16.5 bar	0.34 (Thermal) 26 (Electrical)
Rogdakis and Antonopoulos [46]	Simulation	Aqua-ammonia	Continuous operation	300–1100 kJ/kg	130 to 180	15 to 35	30 to 30	−70 to −30	15 bar	0.2–0.65
Bayramoglu and Bulgan [47]	Simulation	Aqua-ammonia	Continuous operation	1000 kW	110 (Heat source temperature)	25 (Cooling water temp)	25 (Cooling water temp)	−5	Not reported	Not reported
Misra et al. [48]	Simulation	Aqua-ammonia	Continuous operation	Not reported	155	33.75	37	7.5	15.64 bar	0.25